ESAIM: M2AN 46 (2012) 1247–1273
DOI: 10.1051/m2an/2012003

ESAIM: Mathematical Modelling and Numerical Analysis
www.esaim-m2an.org

ADAPTIVITY AND VARIATIONAL STABILIZATION FOR CONVECTION-DIFFUSION EQUATIONS*

Albert Cohen[1], Wolfgang Dahmen[2] and Gerrit Welper[2]

Abstract. In this paper we propose and analyze stable variational formulations for convection diffusion problems starting from concepts introduced by Sangalli. We derive efficient and reliable *a posteriori* error estimators that are based on these formulations. The analysis of resulting adaptive solution concepts, when specialized to the setting suggested by Sangalli's work, reveals partly unexpected phenomena related to the specific nature of the norms induced by the variational formulation. Several remedies, based on other specifications, are explored and illustrated by numerical experiments.

Mathematics Subject Classification. 65N12, 35J50, 65N30.

Received August 9, 2011. Revised December 3, 2011.
Published online March 27, 2012.

1. Introduction

A notorious obstruction to an accurate and efficient numerical simulation of transport dominated processes is the interplay of transport in competition with diffusion. Its perhaps simplest manifestation is the classical linear convection-diffusion-reaction equation which arises in numerous contexts, in particular, in Oseen-type implicit discretizations of non-stationary incompressible Navier Stokes equations. It also serves as a guiding model when developing subgrid scale concepts such as the "variational multiscale method".

To be specific, we shall be concerned in what follows with the boundary value problem

$$-\epsilon\Delta u + b\cdot\nabla u + cu = f \quad \text{in } \Omega, \quad u = 0 \text{ on } \partial\Omega, \tag{1.1}$$

or rather the corresponding weak formulation: find $u \in H_0^1(\Omega)$ s.t.

$$a_\circ(u,v) := \epsilon\,\langle\nabla u, \nabla v\rangle + \langle b\cdot\nabla u, v\rangle + \langle cu, v\rangle = \langle f, v\rangle\,, \quad v \in H_0^1(\Omega), \tag{1.2}$$

which, under well known conditions, admits a unique solution in $u \in H_0^1(\Omega)$. The central theme of this paper is the interplay between stabilization and adaptivity for problems of this type.

Keywords and phrases. Variational problems, adaptivity, *a-posteriori* error estimators, stabilization.

* *This work has been supported in part by the Priority Program SPP 1324, and by the Transregio TR40, "Technological Foundations for the Design of Thermally and Mechanically Highly Loaded Components of Future Space Transportation Systems", funded by the German Research Foundation.*

[1] Laboratoire Jacques-Louis Lions, Université Pierre et Marie Curie, 4 Place Jussieu, 75005 Paris, France. cohen@ann.jussieu.fr

[2] Institut für Geometrie und Praktische Mathematik, RWTH Aachen, 52056 Aachen, Germany. dahmen@igpm.rwth-aachen.de; welper@igpm.rwth-aachen.de

Article published by EDP Sciences

© EDP Sciences, SMAI 2012

https://doi.org/10.1051/m2an/2012003 Published online by Cambridge University Press

1.1. A conceptual preview

The current understanding of adaptive solution concepts with rigorous convergence and complexity estimates is confined to what we call (X,Y)-*stable* variational problems. By this we mean the following: let $a(\cdot,\cdot) : X \times Y \to \mathbb{R}$ be a bilinear form on a pair of Hilbert spaces X, Y with norms $\|\cdot\|_X, \|\cdot\|_Y$. Given a continuous linear functional $f \in Y'$, the normed dual of Y, find $u \in X$ such that

$$a(u,v) = f(v), \quad v \in Y. \tag{1.3}$$

Here "(X,Y)-stable" means that the operator $A : X \to Y'$, induced by $\langle Au, v\rangle = a(u,v)$, $u \in X, v \in Y$, is a norm-isomorphism, *i.e.*

$$\|A\|_{X\to Y'} \le C_A, \quad \|A^{-1}\|_{Y'\to X} \le 1/\alpha \tag{1.4}$$

holds for some constants $0 < \alpha, C_A < \infty$, independent of possibly varying problem parameters. Thus, the "condition" $\kappa_{X,Y}(A) := \|A\|_{X\to Y'}\|A^{-1}\|_{Y'\to X}$ of the operator is bounded by C_A/α.

An essential consequence of (X,Y)-stability is that errors in the "energy norm" $\|\cdot\|_X$ are bounded from below and above by the *dual norm of the residual*

$$\|A\|^{-1}_{X\to Y'}\|Au_h - f\|_{Y'} \le \|u - u_h\|_X \le \|A^{-1}\|_{Y'\to X}\|Au_h - f\|_{Y'}, \quad u_h \in X_h \subset X. \tag{1.5}$$

Thus, as long as $\kappa_{X,Y}(A)$ is of moderate size the residual bounds the error in a good way. All presently known adaptive methods rely in one way or the other on bounding the residuals $\|Au_h - f\|_{Y'}$ from above and below by sums of local terms whose size suggests further local refinements.

This has been realized so far primarily for symmetric problems that are known to be (X,X)-stable where X is a classical Sobolev space or a product of such [5–7]. In principle, the convection-diffusion equation is in the above sense (H^1_0, H^1_0)-stable, but *not* robustly so, since for dominating convection, *i.e.* when $|b|/\epsilon \gg 1$, the condition behaves essentially like $\kappa_{H^1_0,H^1_0}(A) \sim |b|/\epsilon$, so that the relations (1.5) become useless.

This ill-conditioning already on the *infinite dimensional* level causes (at least) two major problem areas, namely (a) the development of *robust solvers* that are able to solve the finite dimensional systems of equations arising from a given discretization with an efficiency that is, for instance, independent of the parameters ϵ, b, c in (1.2), and (b) the choice of the discretization itself. Although these issues are not independent of each other we focus here exclusively on (b). In this regard, it is well-known that, unless a possibly unrealistically small mesh size (depending on ϵ) is chosen, a standard Galerkin discretization of (1.2) will be unstable. Substantial effort has been spent therefore on the development of *stabilization techniques*. One way is to add artificial diffusion in a consistent way and preferably only along stream lines, in order not to smear the possibly near singular (often anisotropic) features exhibited by the true solution. The perhaps most prominent example is the concept of streamline diffusion *e.g.* in the form of SUPG which in special cases can be understood also *via* the so called bubble function approach [3,4]. In spite of the great success of such concepts it is fair to say that from several perspectives the current state of the art is not completely satisfactory. In particular, the choice of stabilization parameters is still a subtle issue that is not fully understood. This is reflected either by remaining unphysical oscillations in the numerical solution or by smearing solution features too much. In brief, stabilization can ameliorate somewhat but not avoid ill-conditioning.

Some of the known stabilization techniques can be interpreted as mimicking, on a discrete level, a *Petrov-Galerkin* formulation. This suggests to choose already on the *infinite dimensional* level X different from Y which, after all seems natural since the underlying equation is not symmetric. In fact, such norms, giving rise in our terminology to an (X,Y)-stable formulation, have already been used in [19] and in [20,21] for the purpose of error estimators. However, these error estimators have been derived for the SUPG, *not* for a discretization based on the (X,Y)-setting.

The central objective of this paper is to explore (X,Y)-stable weak formulations for the convection diffusion equation (1.1) along with discretizations directly based on them. Our two main principal reasons for thereby proposing an alternative to mesh-dependent (*a-priori*) stabilization techniques may be summarized as follows.

https://doi.org/10.1051/m2an/2012003 Published online by Cambridge University Press

First, it is in our opinion desirable to avoid *mixing of numerical and physical stabilization concepts*. In fact, convection-diffusion equations often arise in connection with the *Variational Multiscale Method* [14, 15] that aims at capturing the effect of unresolved scales on a given macro scale that might entirely depend on the given numerical budget. This still requires at the end of the day solving a possibly convection dominated problem in the range of resolved scales endowed with a correction term that is to capture the effect of the unresolved scales on the resolved macro-scale. It is then unsatisfactory that several stabilization terms are ultimately superimposed.

The second aspect, which is the primary focus of the present research, is to explore the combination of (X, Y)-stability with adaptive solution concepts based on the corresponding (X, Y)-discretizations and the interplay of their *discrete* stability with adaptivity. It was experimentally demonstrated in [8] that an adaptive full multigrid scheme for plain Galerkin discretizations of convection dominated problems lead to perfectly stable solutions as long as layers are resolved. In the present context the stabilizing effect of adaptivity enters in a somewhat different way. (X, Y)-stability comes at a prize, namely the resulting variational formulation involves an inner product $\langle \cdot, \cdot \rangle_{Y'}$ that is not readily numerically accessible. The underlying functional analytic principle is closely related to the work on least squares formulations *e.g.* in [1, 2, 16, 17]. While these developments ultimately require dealing with classical H^{-1}-inner products, we encounter here additional difficulties due to the singularly perturbed nature of the underlying problem (1.1). Moreover, after completion of this paper we became aware of recent related work reported in [10, 11]. It centers on the notion of "optimal test spaces" for Petrov-Galerkin discretizations which is closely related to the functional analytic framework developed below in Section 2. However, it is pursued there in a quite different direction than in the present study.

We propose to introduce an auxiliary variable (on the infinite dimensional level), somewhat in the spirit of mixed formulations, that require solving an auxiliary elliptic problem. The exact solution of this problem corresponds to the perfectly stable formulation. The excess resolution of the discretization of this auxiliary problem, compared with the trial space for the "primal" variable, can be interpreted as the "amount of stabilization". The point now is that efficient and reliable *a-posteriori* bounds for errors in the X-norm allow us to determine the right level of stabilization *adaptively*.

Nevertheless, for certain "natural" specifications of variational formulations, suggested by [19–21], resulting adaptive schemes turn out *not* to give rise to a fixed error reduction. A closer look reveals that this is to a great extent due to the specific nature of the induced norms which is in fact shared by most norms for the analysis of convection-diffusion problems including those used for SUPG-schemes. This issue will be discussed along with possible remedies based on further modifying the variational formulation.

We emphasize that the central objective of this paper is *not* to propose a specific definitive scheme that should deal with these obstructions. In fact, we are content here with simple low order finite elements on isotropic refinements, although it will be clear from the experiments that higher order trial functions in layer regions and anisotropic refinements would ameliorate somewhat the observed adverse effects. However, we prefer here to focus on some principal mechanisms that are in our opinion relevant in this context.

1.2. Layout of the paper

The paper is organized as follows: in Section 2 we describe a general variational framework for convection-diffusion equations covering, in particular, the infinite dimensional setting of [19, 21]. A general strategy is introduced to obtain numerical schemes for such well conditioned formulations. Furthermore, connections with subgrid modeling and the SUPG scheme are discussed. Section 3 focuses on adaptive strategies for the convection-diffusion problem that, on the one hand, provide efficient and reliable adaptive approximations of the solution and, on the other hand, determine a proper amount of stabilization. In Section 4 we analyze why for the "natural" formulations approximate solutions still exhibit strong artifacts on low resolution levels. In Section 5 we propose some remedies based on alternate specifications of the variational framework and illustrate them by numerical tests.

https://doi.org/10.1051/m2an/2012003 Published online by Cambridge University Press

2. A stable elliptic formulation and its discretization

In this section we describe a functional analytic setting motivated by [19,21]. To this end assume $\Omega \subset \mathbb{R}^n$ is a domain, $b \in W^{1,\infty}(\Omega)$, $c \in L_\infty(\Omega)$ with

$$c - \frac{1}{2}\mathrm{div} b \geq \bar{c} \qquad \|b\|_\infty \leq c^* \bar{c} \tag{2.1}$$

where $\bar{c}, c^* \geq 0$ are two constants and c and b are the (possibly variable) coefficients of the convection-diffusion problem (1.2). Under these assumptions it is well known that the bilinear form $a_\circ$ from (1.2) induces an isomorphism $A_\circ : H_0^1(\Omega) \to H^{-1}(\Omega)$ through $\langle A_\circ v, w\rangle = a_\circ(v,w)$ for all $v, w \in H_0^1(\Omega)$. Here and below $\langle\cdot,\cdot\rangle$ always denote the dual pairing induced by the standard L_2-inner product. As mentioned in the introduction the condition number of $A_\circ$, however, deteriorates with increasing Peclet number.

Seeking for (X,Y)-stable variational formulations based on $a_\circ$ means then that both X and Y agree with $H_0^1(\Omega)$ as vector spaces but need to be endowed with different equivalent norms to ensure the desired stability on the infinite dimensional level. However, different variational formulations of (1.1) are conceivable involving different bilinear forms that still yield the solution to (1.1) whenever its regularity admits a classical interpretation. This could, for instance, involve incorporating boundary conditions in a different way.

To facilitate a unified treatment of such options our starting point is the following slightly more general scenario. We assume at this point that we are given a pair of Hilbert spaces $\hat{X}, \hat{Y}$, along with a bilinear form $a(\cdot,\cdot) : \hat{X} \times \hat{Y} \to \mathbb{R}$, such that, for any $f \in \hat{Y}'$, the problem

$$a(u,v) = \langle f, v\rangle\,, \quad v \in \hat{Y}, \tag{2.2}$$

has a unique solution u in $\hat{X}$ that, when being regular enough, solves (1.1). Hence, the operator A, defined by $\langle Av, w\rangle = a(v,w)$, $v \in \hat{X}, w \in \hat{Y}$, is an isomorphism. Again, the specific choice $a(\cdot,\cdot) = a_\circ(\cdot,\cdot)$ where $\hat{X} = \hat{Y} = H_0^1(\Omega)$ may serve as a guiding example. We shall refer to this as the *standard choice*.

2.1. Construction of norms

Our objective is then to find a pair of *equivalent* Hilbert spaces X, Y such that now the operator A has condition number $\kappa_{X,Y}(A)$ equal to one. Here, "equivalent" means that X, Y agree with $\hat{X}, \hat{Y}$, respectively, as vector spaces and that the norms $\|\cdot\|_X, \|\cdot\|_{\hat{X}}$ and $\|\cdot\|_Y, \|\cdot\|_{\hat{Y}}$ are equivalent, respectively. Of course, the norms $\|\cdot\|_X$, $\|\cdot\|_Y$ must then involve the problem parameters ϵ, c and b. For the standard choice $\hat{X} = \hat{Y} = H_0^1(\Omega)$ the construction essentially follows the approach in [19,21]. It is also closely related to the least squares approach in [16,17].

We denote by $\langle\cdot,\cdot\rangle_X = \langle\cdot, R_X\cdot\rangle$ and $\langle\cdot,\cdot\rangle_Y = \langle\cdot, R_Y\cdot\rangle$ the respective scalar products where R_X and R_Y are the corresponding Riesz maps.

The general procedure can be described as follow: fix a Hilbertian norm $\|\cdot\|_Y$ on $\hat{Y}$ (as a vector space). Then for any other norm $\|\cdot\|_X$, which is also equivalent to $\|\cdot\|_{\hat{X}}$, the operator A, defined above, is still an isomorphism from X onto Y'. Therefore, the problem (2.2) with $\hat{X}, \hat{Y}$ replaced by X, Y, respectively, is equivalent to

$$\langle Au, Av\rangle_{Y'} = \langle f, Av\rangle_{Y'}\,, \quad v \in X. \tag{2.3}$$

Note that the dual norm $\|\cdot\|_{Y'}$ and inner product $\langle\cdot,\cdot\rangle_{Y'}$ are determined from the choice of the primal norm $\|\cdot\|_Y$. In particular, we have

$$\langle v, w\rangle_{Y'} = \left\langle v, R_Y^{-1} w\right\rangle = \left\langle R_Y^{-1} v, w\right\rangle. \tag{2.4}$$

Choosing now the X-scalar product as

$$\langle v, w\rangle_X := \langle Av, Aw\rangle_{Y'}\,, \quad v, w \in X, \tag{2.5}$$

we have

$$\|v\|_X^2 = \|Av\|_{Y'}^2, \tag{2.6}$$

which means that (1.5) holds with $\|A\|_{X\to Y'} = \|A^{-1}\|_{Y'\to X} = 1$ and (2.3) is perfectly conditioned.

https://doi.org/10.1051/m2an/2012003 Published online by Cambridge University Press

Remark 2.1. Obviously, (2.3) is the normal equation for the infinite dimensional least squares problem

$$u = \mathrm{argmin}_{v\in X}\|Av - f\|_{Y'}. \tag{2.7}$$

Moreover, for any subspace $X_h \subseteq X$ one has

$$u_h = \mathrm{argmin}_{v_h\in X_h}\|u - u_h\|_X \iff u_h = \mathrm{argmin}_{v_h\in X_h}\|f - Au_h\|_{Y'}, \tag{2.8}$$

and replacing X by X_h in (2.3), this variational problem is the normal equation for the least squares problem (2.8), see also [16, 17].

Following [18, 21], a canonical, but by no means mandatory choice for $\|\cdot\|_Y$ is obtained by splitting the original form $a(\cdot,\cdot)$ into its symmetric and skew-symmetric parts

$$a_s(u,v) := \frac{1}{2}\big(a(u,v) + a(v,u)\big), \qquad a_{sk}(u,v) := \frac{1}{2}\big(a(u,v) - a(v,u)\big),$$

which gives

$$a(v,w) = a_s(v,w) + a_{sk}(v,w) =: \langle A_s v, w\rangle + \langle A_{sk} v, w\rangle, \quad (v,w)\in X\times Y, \tag{2.9}$$

where, in particular,

$$A_{sk}^* = -A_{sk} \quad \text{so that} \quad a_{sk}(v,v) = 0 \quad \text{and } A = A_s + A_{sk}. \tag{2.10}$$

For the standard choice of vector spaces X, Y, taking

$$\|y\|_Y^2 := a_s(y,y), \tag{2.11}$$

this norm is indeed equivalent to $\|\cdot\|_{H^1(\Omega)}$ and the corresponding Riesz map is $R_Y = A_s$. Specifically, for problem (1.2) and $a(\cdot,\cdot) = a_\circ(\cdot,\cdot)$ one obtains

$$\langle v,w\rangle_Y := \langle A_s v, w\rangle = \epsilon\,\langle \nabla v, \nabla w\rangle + \left\langle (c - \frac{1}{2}\mathrm{div}(b)v, w\right\rangle. \tag{2.12}$$

Note that in this case (2.6), by cancellation of the skew-symmetric term, takes the form

$$\|v\|_X^2 = \|v\|_Y^2 + \|A_{sk}v\|_{Y'}^2. \tag{2.13}$$

The main obstacle for an implementation of the scheme (2.3) is that in general the Y' norm is a dual norm so that the scalar product cannot easily be evaluated. This issue is addressed in the next section.

2.2. Resolving the Y'-scalar product

Noting that

$$\|R_Y v\|_{Y'} = \|v\| \quad \text{and} \quad \|w\|_{Y'} = \|R_Y^{-1} w\|_Y, \tag{2.14}$$

and recalling the explicit formula (2.4) for the Y'-scalar product, the variational problem (2.3) can be restated as

$$\left\langle Au - f, R_Y^{-1} Av\right\rangle = 0, \quad v\in X, \tag{2.15}$$

which is now based on the standard dual pairing between Y and Y' but involves the inverse of R_Y. Recall that this dual pairing reduces to a regular L_2-inner product in case u and f are sufficiently smooth. Before we proceed note that this variational formulation is essentially an (infinite dimensional) Petrov-Galerkin formulation with the ideal test space $R_Y^{-1}AX$. However, introducing an auxiliary variable

$$y = R_Y^{-1}(Au - f) \quad \Leftrightarrow \quad R_Y y - Au = -f,$$

https://doi.org/10.1051/m2an/2012003 Published online by Cambridge University Press

the problem (2.15) is equivalent to finding $(u, y) \in X \times Y$ such that

$$\begin{aligned} \langle y, Av\rangle &= 0, \qquad v \in X, \\ \langle Au, z\rangle - \langle R_Y y, z\rangle &= \langle f, z\rangle, \quad z \in Y. \end{aligned} \tag{2.16}$$

Thus, at the expense of an additional variable y we arrive at a variational problem that could be treated, for instance, by standard finite element discretizations. First let us confirm though that the system (2.16) is well posed. To this end, let

$$\bar{a}([u, y], [v, z]) := \langle y, Av\rangle + \langle Au, z\rangle - \langle R_Y y, z\rangle, \tag{2.17}$$

which is the bilinear form $\bar{a} : (X \times Y) \times (X \times Y) \to \mathbb{R}$ corresponding to (2.16).

Proposition 2.2. *The bilinear form* (2.17) *defines an isomorphism* $\bar{A} : (X \times Y') \to (X' \times Y')$ *with the mapping property*

$$\frac{1}{\sqrt{3}} \|\bar{A}[u, y]\|_{X' \times Y'} \le \|[u, y]\|_{X \times Y} \le \sqrt{3} \|\bar{A}[u, y]\|_{X' \times Y'}. \tag{2.18}$$

Proof. We denote by $\bar{A} : X \times Y \to X' \times Y'$ the operator corresponding to the bilinear form (2.17). We have to show that this operator is an isomorphism. To this end we consider the equation $\bar{A}[u, y] = [g, f]$. According to (2.16) this is equivalent to the following system

$$\begin{aligned} A^* y &= g \\ Au - R_Y y &= f. \end{aligned} \tag{2.19}$$

To see that this system possesses a unique solution, recall that $A^* : Y \to X'$ is an isomorphism. Therefore $y := A^{-*} g := (A^*)^{-1} g$ satisfies the first row of the system. Furthermore, since $A : X \to Y'$ is an isomorphism we infer from the second row $u = A^{-1}(f - R_Y y)$, showing that (2.19) has a solution.

To show its uniqueness we prove that the operator $\bar{A}$ has a trivial kernel. To this end, assume $\bar{A}[u, y] = 0$. Again by the first row of (2.19) we get $y = 0$. Plugging this into the second row yields $Au = 0$ which implies $u = 0$. Thus, $\bar{A}$ is injective.

Now one can explicitly write down the inverse of $\bar{A}$ which is given by

$$\bar{A}^{-1}[g, f] = [A^{-1}(f - R_Y A^{-*} g), A^{-*} g]. \tag{2.20}$$

Finally we have to show that the norms of $\bar{A}$ and its inverse $\bar{A}^{-1}$ are bounded. First we get

$$\|\bar{A}[u, y]\|^2_{X' \times Y'} = \|A^* y\|^2_{X'} + \|Au - R_Y y\|^2_{Y'} \le 2\|u\|^2_X + 3\|y\|^2_Y, \tag{2.21}$$

where we have used the definition $\|u\|_X = \|Au\|_{Y'}$ of the X-norm and its consequence $\|A^* y\|_{X'} = \|y\|_Y$. Finally, by the explicit formula (2.20) for the inverse, we obtain, again using $\|A^{-*} g\|_Y = \|g\|_{X'}$,

$$\begin{aligned} \|\bar{A}^{-1}[g, f]\|^2_{X \times Y} &= \|A^{-1}(f - R_Y A^{-*} g)\|^2_X + \|A^{-*} g\|^2_Y \\ &\le \|f - R_Y A^{-*} g\|^2_{Y'} + \|g\|^2_{X'} \le 2\|f\|^2_{Y'} + 3\|g\|^2_{X'}. \end{aligned} \tag{2.22}$$

□

We conclude this section with the simple observation that the above strategy of first prescribing Y and then choosing X through setting $\|v\|_X := \|Av\|_{Y'}$ can be reversed which is the point of view taken in [9] for a different problem class. In fact, first prescribing X and setting $\|y\|_Y = \|A^* y\|_{X'}$ yields the dual space $\|f\|_{Y'} = \|A^{-1} f\|_X$ so that one obtains again the desired mapping property $\|Au\|_{Y'} = \|u\|_X$ and (X, Y)-stability with perfect condition $\kappa_{X,Y}(A) = 1$.

https://doi.org/10.1051/m2an/2012003 Published online by Cambridge University Press

2.3. Discretization and stabilization

As in the case of the infinite dimensional convection-diffusion problem (1.1) we always assume that for any $X_h \subseteq X$

$$a(u_h, v_h) = 0,\ v_h \in X_h \quad \Rightarrow \quad u_h = 0. \tag{2.23}$$

The problem (2.16), or equivalently

$$\bar{a}([u, y], [v, z]) = \langle f, z\rangle\,, \quad [v, z] \in X \times Y, \tag{2.24}$$

can be treated in the usual way. Specifically, suppose that $X_h \subset X$ and $Y_h \subset Y$ are finite dimensional trial spaces for the two solution components. To understand the roles of X_h and Y_h with regard to the stability of the discretization, note first that the resulting finite dimensional problem

$$\bar{a}([u_h, y_h], [v_h, z_h]) = \langle f, z_h\rangle\,, \quad [v_h, z_h] \in X_h \times Y_h, \tag{2.25}$$

or equivalently written as a block system,

$$\begin{array}{rl} \langle y_h, Av_h\rangle = 0, & v_h \in X_h \\ \langle Au_h, z_h\rangle - \langle R_Y y_h, z_h\rangle = \langle f, z_h\rangle\,, & z_h \in Y_h, \end{array} \tag{2.26}$$

could, in principle, be very ill-conditioned. In fact, consider first the case $X_h = Y_h$. Testing with $[v_h, 0]$, $v_h \in Y_h = X_h$, reveals that, by (2.23), $y_h = 0$, which, by testing with $[0, z_h]$ gives $a(u_h, z_h) = \langle f, z_h\rangle$, $z_h \in Y_h = X_h$. This is simply the original Galerkin discretization which is unstable. On the other hand, choosing for any finite dimensional $X_h \subset X$ the second component as the whole infinite dimensional space Y, and calling the resulting solution $[u_h, \hat{y}_h]$, we can redo the steps (2.15) to (2.16) for the derivation of the block system. Namely setting v_h to zero gives $\hat{y}_h = R_Y^{-1}(Au_h - f)$. Plugging this again into the discrete system (2.25) and setting $z_h = 0$ gives the original least squares problem

$$\langle Au_h - f, Av_h\rangle = 0, \quad v_h \in X_h$$

which by Remark 2.1 gives the optimal discrete approximation in the X-norm.

In summary, the same discretization for both components u and y is unstable while an infinite resolution for the auxiliary variable y gives rise to a stable formulation with condition equal to one. This suggests that the excess resolution of y relative to u acts as a *stabilization*.

That raises two questions: (i) can we find *a-priori* criteria to determine how large should Y_h be for a given X_h, or more generally, how Y_h should be related to X_h to warrant uniform stability of the discrete problems? (ii) are there practical *a-posteriori* error indicators that tell us at any given stage how much stabilization is needed to warrant a desired target accuracy of an approximate solution? This would give rise to another manifestation of adaptivity as a stabilizing concept. We defer (i) and address (ii) in Section 3.3 below.

2.4. Subgrid modeling and SUPG

Next we briefly pause to put the above numerical scheme into the context of subgrid modeling and compare it to the SUPG scheme.

Accepting the fact that turbulent flows involve a range of relevant scales that can usually not be resolved by a numerical scheme, one may try to still capture the effect of unresolved scales on the macro scale by modeling them. Examples are low parameter models, large Eddy simulation or modern variants such as variational multiscale method and subgrid modeling. As pointed out in [12,13] all these approaches may be interpreted as *regularizing* the Navier Stokes equations. It is therefore perhaps interesting to see how this fits into the present setting. To this end, let $X_h \subset X$ be again a finite dimensional trial space while in general Y_h should be a larger space which, for simplicity of exposition is for the moment taken to be all of Y. This is the second scenario

https://doi.org/10.1051/m2an/2012003 Published online by Cambridge University Press

considered in the previous subsection leading to a conceptually stable formulation for the semi-discrete problem on $X_h \times Y$.

Next we assume that $X_h \subset Y$ which is of course true for the above choice $X = Y = H_0^1(\Omega)$ endowed with suitably modified norms. In order to interpret the scheme (2.26) in terms of subgrid modeling consider its first row. Defining the Galerkin projection $P_h : Y \to X_h$ by

$$a(v_h, P_h z - z) = 0, \quad v_h \in X_h, \tag{2.27}$$

it states that $P_h \hat{y}_h = 0$, *i.e.* $\hat{y}_h$, defined in the previous subsection, is a *fluctuation* in nature. In order to use this observation in the second row of (2.26) we first decompose the space Y into

$$Y = P_h \oplus (I - P_h)Y = X_h \oplus X_h^\perp.$$

Now we can split the test functions of (2.26) into test functions from X_h and from $X_h^\perp$ which gives

$$\begin{aligned} \langle Au_h, z_h\rangle - \langle R_Y \hat{y}_h, z_h\rangle &= \langle f, z_h\rangle, \quad z_h \in X_h \\ - \langle R_Y \hat{y}_h, z_h\rangle &= \langle f, z_h\rangle, \quad z_h \in X_h^\perp, \end{aligned}$$

where we have used that $\langle Au_h, z_h\rangle = 0$ for all $z_h \in X_h^\perp$. In this equation we can interpret the first row as a plain Galerkin scheme with a correction $-\langle R_Y \hat{y}_h, z_h\rangle$. Since $P_h \hat{y}_h = 0$ this represents essentially the influence of the unresolved scales on the resolved scales.

In order to compare the scheme (2.25) with the SUPG scheme we first rewrite the least squares problem (2.3) in a slightly different form. To this end, for the choice $R_Y = A_s$ with the decomposition $A = A_s + A_{sk}$, we observe that by (2.4) and (2.11), the least squares problem (2.3) takes the form

$$\langle Au, v\rangle + \langle Au, A_{sk} v\rangle_{Y'} = \langle f, v\rangle + \langle f, A_{sk} v\rangle_{Y'}, \quad v \in X_h. \tag{2.28}$$

Note that the stabilization terms added in SUPG could be viewed as mimicking the terms $\langle Au, A_{sk} v\rangle_{Y'}$ and $\langle f, A_{sk} v\rangle_{Y'}$ by suitably weighted element-wise defined inner products. However, while SUPG stabilization does *not* give rise to variational formulations with uniformly bounded condition numbers, the formulation (2.28) does.

3. Adaptive strategies

In this section we investigate adaptive strategies for the system (2.26). To be specific, we confine the discussion in this section to the standard choice $a(\cdot,\cdot) = a_\circ(\cdot,\cdot)$ given by (1.2) with X, Y both being equivalent to $H_0^1(\Omega)$.

The reason for adaptivity for this problem is twofold. On the one hand, solutions of convection-diffusion problems typically have layers which we wish to resolve adaptively. On the other hand, we have already seen in Section 2.3 that the resolution of the auxiliary variable y determines the amount of stabilization which therefore opens the door for steering stabilization through adaptation.

To keep this article self contained we briefly recall in the next section the error estimators from [21]. Based on those estimators we derive in the Section 3.2 *a-posteriori* error estimators for the block system (2.26). Then, we deduce in Section 3.3 suitable *a-posteriori* conditions for stability and present in Section 3.4 a short numerical experiment.

3.1. The error estimators of Verfürth

In order to apply the error estimators from [21] we choose $R_Y = A_s$ throughout this section. Recall that for this choice we have the norms

$$\|v\|_Y^2 = a(v, v), \qquad \|v\|_X^2 = \|Av\|_{Y'}^2.$$

https://doi.org/10.1051/m2an/2012003 Published online by Cambridge University Press

Then the model problem treated in [21] is: find $y_h \in Y_h$ s.t.

$$\langle R_Y y_h, z_h\rangle = \langle f - Au_h, z_h\rangle\,, \quad z_h \in Y_h. \tag{3.1}$$

This problem is, of course, the second block row of (2.16) or rather the discrete case (2.25). In this section we treat u_h as a fixed function. In the next section we use this estimator for the full system where also u_h is an unknown variable. This setting is slightly more general than the results in [21] because in this paper only right hand sides, which are piecewise constant on a finite element grid, are allowed. However the statements of this section with this more general right hand side can be proved in identical ways.

To state the main result of [21] we first need some notation. So far we have not considered the type of finite dimensional spaces for X_h and Y_h. In this section we will fix it to finite element spaces. To this end let $\mathcal{T}_h^X$, $\mathcal{T}_h^Y$ be admissible and shape regular triangulation and $\mathcal{E}_h^X$, $\mathcal{E}_h^Y$ be the corresponding set of edges. Then X_h and Y_h are the corresponding finite element space

$$X_h = \{u \in H_0^1(\Omega) :\, u|_T \in \mathcal{P}^k,\, T \in \mathcal{T}_h^X\}$$
$$Y_h = \{y \in H_0^1(\Omega) :\, y|_T \in \mathcal{P}^l,\, T \in \mathcal{T}_h^Y\}$$

of continuous piecewise polynomial function of degree k and l respectively. For any edge E, we denote by n_E a unit normal vector. If $E = T^+ \cap T^-$ and if n_E points towards the element T^+ we denote by

$$[F]_E = n_E \cdot F^+_{|E} - n_E \cdot F^-_{|E},$$

the jump accross E of a piecewise continuous vector field F, where F^+ and F^- are its restriction to T^+ and T^- respectively.

In order to be able to apply the theory from [21] we have to assume that the spaces X_h and Y_h are nested, *i.e.* $X_h \subset Y_h$. The reason is the appearance of the variable u_h in the right hand side. Because for the error estimators we are mainly concerned with the finite element space Y_h we will usually drop the superscript ^{Y}. Next define

$$\alpha_S := \min\{\epsilon^{-1/2} h_S, \bar{c}^{-1/2}\}, \quad S \in \{T, E\},\ h_S := \operatorname{diam} S, \tag{3.2}$$

where $\bar{c}$ is the constant from (2.1). Here the diameters h_S and cells T and E might correspond to either triangulation $\mathcal{T}_h^X$ or $\mathcal{T}_h^Y$ which will be clear from the context.

Along the lines of [21] we now define the element and edge residuals

$$\begin{aligned}\rho_T(u_h, y_h) &:= f - Au_h + R_Y y_h|_T \\ &= \left(f + \epsilon\Delta(u_h - y_h) - b\nabla u_h + c(y_h - u_h) - \frac{1}{2}\operatorname{div}(b) y_h\right)\Big|_T \end{aligned} \tag{3.3}$$

$$\rho_E(u_h, y_h) := \begin{cases} \epsilon[\nabla(y_h - u_h)]_E & \text{if } E \not\subset \Gamma, \\ 0 & \text{if } E \subset \Gamma. \end{cases} \tag{3.4}$$

Next we define an error indicator for one element T by

$$\eta_T(u_h, y_h, T)^2 := \alpha_T^2 \|\rho_T(u_h, y_h)\|^2_{0;T} + \epsilon^{-1/2}\alpha_E \|\rho_{\partial T}(u_h, y_h)\|^2_{0;\partial T} \tag{3.5}$$

as well as for a set $\mathcal{T}' \subset \mathcal{T}_h$ of elements by

$$\eta_{\mathcal{T}_h}(u_h, y_h, \mathcal{T}')^2 = \sum_{T \in \mathcal{T}'} \eta_{\mathcal{T}_h}(u_h, y_h, T)^2.$$

Finally we define the data error

$$osc(f, \mathcal{T}_h^Y)^2 = \inf_{z_h \in Y_h} \|f - z_h\|^2_{Y'}, \tag{3.6}$$

where errors in b and c are excluded for simplicity. Then one gets from [21] the following theorem.

https://doi.org/10.1051/m2an/2012003 Published online by Cambridge University Press

Theorem 3.1. *Assume that the error indicators $\eta(u_h, y_h, T)$ and the data errors $osc(f, \mathcal{T}_h^Y)$ are defined as in (3.5) and (3.6) respectively. Furthermore assume that $X_h \subset Y_h$. Then we have the upper bound*

$$\|\hat{y} - y_h\|_Y^2 \leq \eta(u_h, y_h, \mathcal{T}_h^Y)^2 + osc(f, \mathcal{T}_h^Y)^2$$

and the lower bound

$$\eta(u_h, y_h, \mathcal{T}_h^Y)^2 \leq \|\hat{y} - y_h\|_Y^2 + osc(f, \mathcal{T}_h^Y)^2$$

where $\hat{y}$ is the solution of (3.1) with $Y_h = Y$ for fixed $u_h \in X_h$.

3.2. Error estimators for the block system

In this section we analyze *a-posteriori* error estimators for the full discrete system

$$\bar{a}([u_h, y_h], [v_h, z_h]) = \langle f, z_h \rangle, \quad [v_h, z_h] \in X_h \times Y_h, \tag{3.7}$$

with the choice $R_Y = A_s$. Especially we want to derive efficient and reliable bounds for the error

$$\|u - u_h\|_X^2 + \|y - y_h\|_Y^2 = \|u - u_h\|_X^2 + \|y_h\|_Y^2, \tag{3.8}$$

where we have used that $y = R_Y^{-1}(Au - f) = 0$ holds for the solution u of (2.2). Moreover, since by (2.6) we have $\|u - u_h\|_X = \|A(u - u_h)\|_{Y'} = \|f - Au_h\|_{Y'}$, the term we need to estimate is just

$$\|Au_h - f\|_{Y'}^2 + \|y_h\|_Y^2. \tag{3.9}$$

The second summand is already a computable quantity. However, it is always dominated by the first summand in (3.9). In fact, choosing $v_h = 0$ in (3.7) implies

$$\langle R_Y y_h, z_h \rangle = a(u_h, z_h) - \langle f, z_h \rangle = \langle Au_h - f, z_h \rangle,$$

so that by standard reasoning

$$\begin{aligned} \|y_h\|_Y &= \frac{\langle R_Y y_h, y_h \rangle}{\|y_h\|_Y} = \sup_{z_h \in Y_h} \frac{\langle R_Y y_h, z_h \rangle}{\|z_h\|_Y} \\ &= \sup_{z_h \in Y_h} \frac{\langle Au_h - f, z_h \rangle}{\|z_h\|_Y} \leq \sup_{z \in Y} \frac{\langle Au_h - f, z \rangle}{\|z\|_Y} \\ &= \|Au_h - f\|_{Y'}, \end{aligned} \tag{3.10}$$

which therefore gives for any $Y_h \subseteq Y$

$$\|Au_h - f\|_{Y'}^2 \leq \|u - u_h\|_X^2 + \|y - y_h\|_Y^2 \leq 2\|Au_h - f\|_{Y'}^2. \tag{3.11}$$

Again it is instructive to look at the following two choices of Y_h. If $Y_h = X_h$ we have $y_h = 0$ which corresponds to an unstable discretization. Nonetheless, the *a-posteriori* indicators from [20, 21] would yield sharp lower and upper bounds for $\|Au_h - f\|_{Y'}$. This may, however, not give useful information for refinements since these indicators reflect also the unphysical oscillations in regions where no refinement would be needed. The other extreme case is $Y_h = Y$. Then (3.10) actually gives

$$\|y_h\|_Y = \|Au_h - f\|_{Y'} \quad \text{whenever} \quad Y_h = Y. \tag{3.12}$$

Hence in the "stable" situation both terms in the error representation (3.9) are the same. Thus a reasonable refinement strategy should aim at balancing both contributions. We take up this point of view again later in connection with a concrete refinement strategy.

https://doi.org/10.1051/m2an/2012003 Published online by Cambridge University Press

Let us now turn to identifying corresponding computable indicators for the error (3.8). Using Galerkin orthogonality one has

$$\bar{a}([u-u_h, y-y_h],[v_h,z_h]) = 0, \quad [v_h,z_h] \in X_h \times Y_h, \tag{3.13}$$

for the discrete solution $[u_h, y_h] \in X_h \times Y_h$ of (3.7) so that we obtain by Proposition 2.2 in the usual manner

$$\left(\|u-u_h\|_X^2 + \|y_h\|_Y^2\right)^{1/2} \leq 3 \sup_{[v,z]\in X\times Y} \frac{\bar{a}([u-u_h,-y_h],[v-v_h,z-z_h])}{\left(\|v\|_X^2+\|z\|_Y^2\right)^{1/2}}. \tag{3.14}$$

Abbreviating $e_r := r - r_h$, $r \in \{u, y, v, z\}$, straightforward calculations yield

$$\begin{aligned} \bar{a}([e_u,-y_h],[e_v,e_z]) &= -\langle y_h, Ae_v\rangle + \langle Ae_u + R_Y y_h, e_z\rangle \\ &= -\langle y_h, Ae_v\rangle + \langle f - Au_h + R_Y y_h, e_z\rangle \\ &= -\langle y_h, Av\rangle + \langle f - Au_h + R_Y y_h, e_z\rangle, \end{aligned} \tag{3.15}$$

where we have used that by (3.7)

$$\langle y_h, Av_h\rangle = 0, \quad v_h \in X_h. \tag{3.16}$$

Now with Theorem 3.1 we can estimate

$$|\langle f - Au_h + R_Y y_h, e_z\rangle| \leq C\eta_{\mathcal{T}}(u_h,y_h,\mathcal{T}')\|z\|_Y + osc(f,\mathcal{T}_h^Y)\|z\|_Y. \tag{3.17}$$

Moreover,by (2.5), we have

$$|\langle y_h, Av\rangle| \leq \|y_h\|_Y \|Av\|_{Y'} = \|y_h\|_Y\|v\|_X. \tag{3.18}$$

Thus combining (3.17), (3.18) and (3.15), yields

$$\begin{aligned} |\bar{a}([e_u,e_y],[e_v,e_z])| &\leq C\|y_h\|_Y\|v\|_X + \eta_{\mathcal{T}}(u_h,y_h,\mathcal{T})\|z\|_Y + osc(f,\mathcal{T}_h^Y)\|z\|_Y \\ &\leq C'\left(\|y_h\|_Y^2 + \eta_{\mathcal{T}}(u_h,y_h,\mathcal{T})^2 + osc(f,\mathcal{T}_h^Y)^2\right)^{1/2}\left(\|v\|_X^2+\|z\|_Y^2\right)^{1/2}. \end{aligned} \tag{3.19}$$

Thus, we can infer from (3.14) that

$$\|u-u_h\|_X^2 + \|y-y_h\|_Y^2 \leq C\left(\|y_h\|_Y^2 + \eta_{\mathcal{T}}(u_h,y_h,\mathcal{T})^2 + osc(f,\mathcal{T}_h^Y)^2\right). \tag{3.20}$$

Note that $\|y_h\|_Y^2 + \eta_{\mathcal{T}}(u_h,y_h,\mathcal{T}')^2$ are computable and in fact localizable quantities that can, in principle, be used for steering adaptive refinements for both X_h and Y_h.

In view of (3.10) and (3.11), to derive lower bounds, it suffices to show that $\eta_{\mathcal{T}}(u_h,y_h,\mathcal{T}')^2$ is bounded by a constant multiple of $\|u-u_h\|_X^2 + \|y_h\|^2$ plus data oscillations. That this is indeed the case follows from Theorem 3.1 which yields

$$\eta(u_h,y_h,\mathcal{T}_h^Y)^2 \leq \|\hat{y}-y_h\|_Y^2 + osc(f,\mathcal{T}_h^Y)^2.$$

Now we can use that $\|\hat{y}\| = \|R_Y^{-1}(Au-Au_h)\|_Y = \|u-u_h\|_X$ which gives

$$\eta(u_h,y_h,\mathcal{T}_h^Y)^2 \lesssim \|u-u_h\|_X^2 + 2\|y_h\|_Y^2 + osc(f,\mathcal{T}_h^Y)^2$$

as desired.

In summary we therefore obtain the following result.

Proposition 3.2. *In the above terms one has for a uniform constant C*

$$\|u-u_h\|_X^2 + \|y_h\|_Y^2 \leq C(\eta(u_h,y_h,\mathcal{T}_h^Y)^2 + osc(f,\mathcal{T}_h^Y)^2),$$

as well as

$$\eta(u_h,y_h,\mathcal{T}_h^Y)^2 \leq C(\|u-u_h\|_X^2 + \|y_h\|_Y^2 + osc(f,\mathcal{T}_h^Y)^2).$$

https://doi.org/10.1051/m2an/2012003 Published online by Cambridge University Press

3.3. Adaptive stabilization

When trying to use the above error indicators for steering an adaptive refinement process, it is not quite clear how exactly should one treat the terms involving the auxiliary variable y relative to the terms involving u. In fact, as we have already seen in Section 2.3, the resolution of the space Y_h in relation to X_h determines the level of stabilization. The following lemma gives a sufficient condition for Y_h to ensure a stable discretization.

Lemma 3.3. *Assume $u_h \in X_h$ and $y_h \in Y_h$ are solutions of the scheme (2.26) and that for some fixed $\delta \in (0,2)$ we have*

$$\|R_Y^{-1}(Au_h - f) - y_h\|_Y \leq \delta \|y_h\|_Y. \tag{3.21}$$

Then we get

$$\|u - u_h\|_X + \|y - y_h\|_Y \leq 4\left(1 - \frac{\delta}{2}\right)^{-2} \inf_{\phi \in X_h} \|u - \phi\|_X. \tag{3.22}$$

Before proving this lemma, some comments on assumption (3.21) are in order. Recall that for a fixed u_h the corresponding auxiliary variable y_h is given by the variational problem

$$\langle Au_h, z_h\rangle - \langle R_Y y_h, z_h\rangle = \langle f, z_h\rangle \tag{3.23}$$

for all $z_h \in Y_h$. Thus y_h is the Y-orthogonal projection of the exact infinite dimensional solution $\hat{y}_h = R_Y^{-1}(Au_h - f)$, *i.e.* it is a Galerkin approximation for the elliptic variational problem $\langle R_Y \hat{y}_h, z\rangle = \langle Au_h, z\rangle - \langle f, z\rangle$. Therefore, we can apply the *a-posteriori* error estimators from [20,21] to control the left hand side of (3.21). Furthermore, the right hand side of (3.21) can be computed explicitly. Thus, one can check *a-posteriori* whether the resolution of Y_h is sufficiently high and, if necessary, refine the grid of Y_h.

Also note that despite the fact that we have two variables u and y the overall error is governed by the approximation error of u alone. Intuitively this is reasonable because the approximation error $\inf_{\varphi \in Y_h} \|y - \varphi\|_Y = 0$ because $y = 0$.

Proof of Lemma 3.3. We employ the following abbreviations

$$\begin{aligned} e_u &= u - u_h & e_y &= y - y_h \\ d_u &= u - P_{X_h} u & d_y &= y - P_{Y_h} y, \end{aligned}$$

and as before

$$\hat{y}_h = R_Y^{-1}(Au_h - f) = -R_Y^{-1} A e_u,$$

where P_{X_h} and P_{Y_h} are the X and Y orthogonal projectors onto X_h and Y_h, respectively, *i.e.* d_u and d_y are the residuals of the best approximation, respectively.

With the definition (2.5) of the X-norm we may proceed as in the proof of the Céa lemma.

$$\|e_u\|_X^2 = \langle Ae_u, Ae_u\rangle_{Y'} = -\langle Ae_u, \hat{y}_h\rangle = -\langle Ae_u, y_h\rangle + \langle Ae_u, y_h - \hat{y}_h\rangle$$

and using the second block row of (2.26) we have

$$\|e_y\|_Y^2 = \langle R_Y y_h, y_h\rangle = \langle Au_h - f, y_h\rangle = -\langle Ae_u, y_h\rangle .$$

This yields

$$\|e_u\|_X^2 + \|e_y\|_Y^2 = -2\langle Ae_u, y_h\rangle + \langle Ae_u, y_h - \hat{y}_h\rangle . \tag{3.24}$$

Using Galerkin orthogonality in the first block row of (2.26), we obtain $\langle Ae_u, y_h\rangle = \langle Ad_u, y_h\rangle$. Furthermore, by the assumption (3.21) we have

$$\|y_h - \hat{y}_h\|_Y \leq \delta \|y_h\|_Y = \delta \|e_y\|_Y,$$

https://doi.org/10.1051/m2an/2012003 Published online by Cambridge University Press

where we have used that $y = 0$. Thus, with (3.24) and (2.6) we conclude that

$$\|e_u\|^2 + \|e_y\|^2 \leq 2\|d_u\|_X \|e_y\|_Y + \delta \|e_u\|_X \|e_y\|_Y.$$

Now Young's inequality $ab \leq \frac{1}{2c}a^2 + \frac{c}{2}b^2$ with $c = \frac{1}{2}\left(1 - \frac{\delta}{2}\right)$ for the first summand and $c = 1$ for the second summand of the right hand side yields the desired error estimate (3.22) for $\delta < 2$. □

The above observations suggest now the following organization of typical adaptive refinement cycle

$$solve \rightarrow estimate \rightarrow refine$$

for the numerical solution of the system (2.16) regarding proper refinements of the two individual spaces X_h and Y_h. As we have already seen in (3.11) the error $\|y - y_h\|_Y$ of the auxiliary variable is always bounded by the error $\|u - u_h\|_X$ of the solution. Thus, in the $solve \rightarrow estimate \rightarrow refine$ cycle we use the estimator $\eta(u_h, y_h, \mathcal{T})$ only to refine the grid of X_h. As we have argued above we only expect a stable scheme if Y_h is somewhat more refined than X_h. The simplest strategy is to generate the new grid for Y_h by refining all cells of the grid $\mathcal{T}$ of X_h a fixed number of times. In our experiments two refinement levels have always been sufficient. The following more sophisticated variant is suggested by Lemma 3.3. After each refinement of X_h one sets first $Y_h = X_h$. Surely this will not give rise to a stable scheme. Now one can use an inner $solve \rightarrow estimate \rightarrow refine$ cycle to refine the grid Y_h until the condition (3.21) is satisfied. The complete algorithm 1 is outlined in Algorithm 1.

Algorithm 1 Adaptive stabilization

```
Choose initial spaces X_h, Y_h.
Choose the stability parameter δ and the error bound ε.
while η(u_h, y_h, T_h^Y) + osc(f, T_h^Y) ≥ ε^2 do
    Compute u_h and y_h by (2.16)
    Compute the estimators η(u_h, y_h, T_h^Y).
    Refine T_h^X by bulk chasing.
    Set T_h^X = T_h^Y.
    while Condition (3.21) not true do
        Compute u_h and y_h by (2.16)
        Estimate ||R_Y^{-1}(Au_h − f) − y_h||_Y.
        Refine T_h^Y by bulk chasing.
    end while
end while
```

3.4. A numerical experiment

As a simple test problem for Algorithm 1 we consider

$$-\epsilon \Delta u + \begin{pmatrix} 1 \\ 1 \end{pmatrix} \cdot \nabla u = 1 \quad \text{in } \Omega = (0,1)^2, \; u = 0 \text{ on } \partial\Omega, \tag{3.25}$$

for $\epsilon = 10^{-5}$. We choose Y as H_0^1 with the norm defined in (2.11) which leads to the according infinite dimensional block system (2.16) or rather (2.24). We apply Algorithm 1 of the last section where we use quadrilateral grids with bilinear finite elements for X_h and Y_h.

The approximate solutions shown in Figure 1 approximately fulfill the partial differential equation in the interior of Ω but miss the boundary conditions completely by introducing a second boundary layer at the inflow part of the boundary.

The bottom part of Figure 1 also shows that there is at most 3 levels of refinement between the grid of Y_h and the grid of X_h. In that sense, the algorithm "succeeds" in ensuring condition (3.21), with Y_h not too much

https://doi.org/10.1051/m2an/2012003 Published online by Cambridge University Press

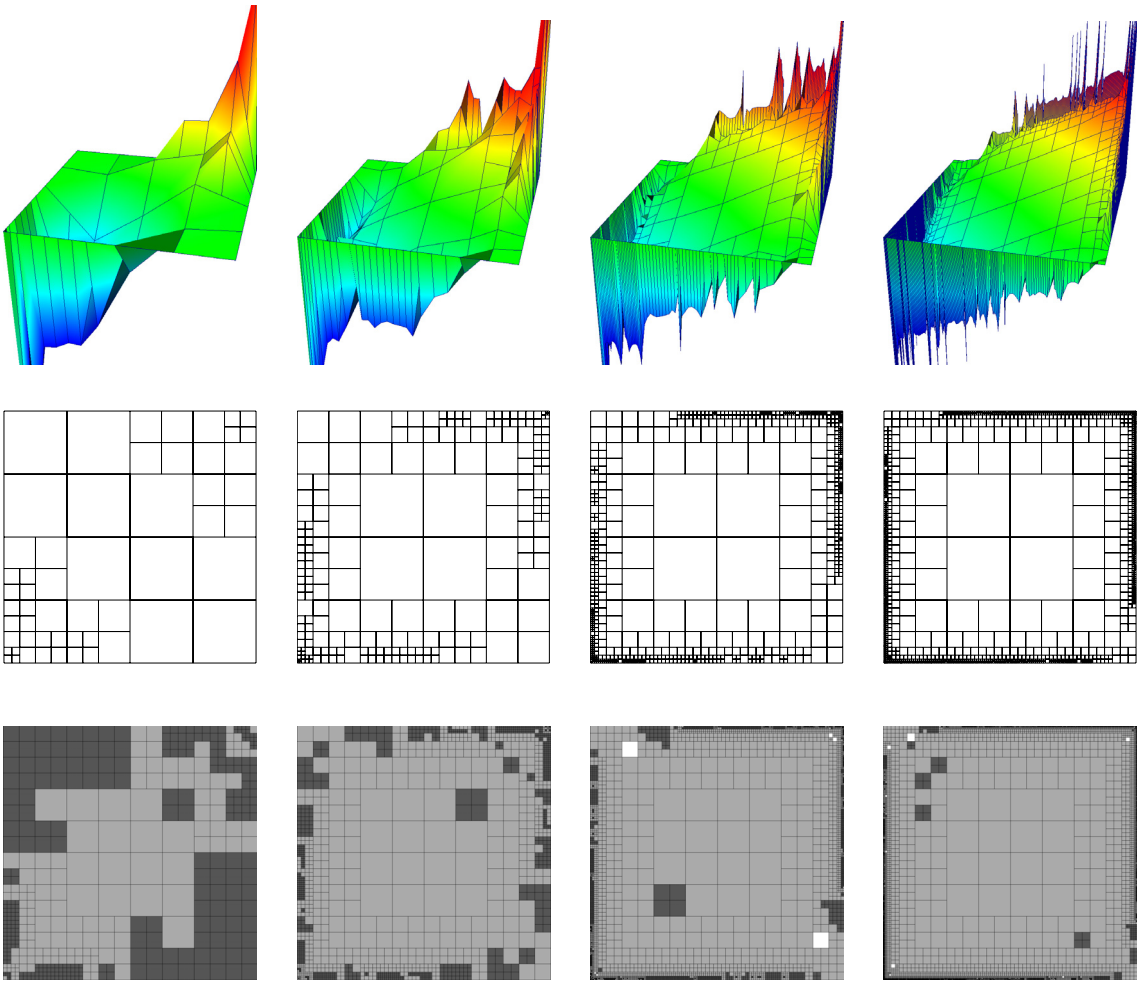


FIGURE 1. These plots show every third adaptive cycle of Algorithm 1 for $\epsilon = 10^{-5}$ starting from cycle 5 for test problem (3.25). The first row depicts the finite element solution u_h. The second row shows the corresponding grid of X_h. The third row shows the local amount j of refinement of the Y_h grid compared to the X_h grid (white $j = 0$, light grey $j = 1$, dark grey $j = 2$, black $j = 3$).

refined compared to X_h, so that the optimal error bound (3.22) must hold. However, this optimal bound does not prevent the numerical solution to behave badly, and we observed that this behaviour persists even when further refining Y_h and letting "tend" to Y.

This test therefore reveals a defect of the X norm defined by (2.13), and which we analyze in more detail in the next section.

4. A CLOSER LOOK AT THE NORMS

In this section we first analyze in more detail why we see the shift artifacts in the numerical examples of Section 3.4. Then in Section 5 we give a motivation for some possible remedies which are discussed in Sections 5.1 and 5.2. Finally some examples for the estimation of drag and lift coefficients are given in Section 5.3.

https://doi.org/10.1051/m2an/2012003 Published online by Cambridge University Press

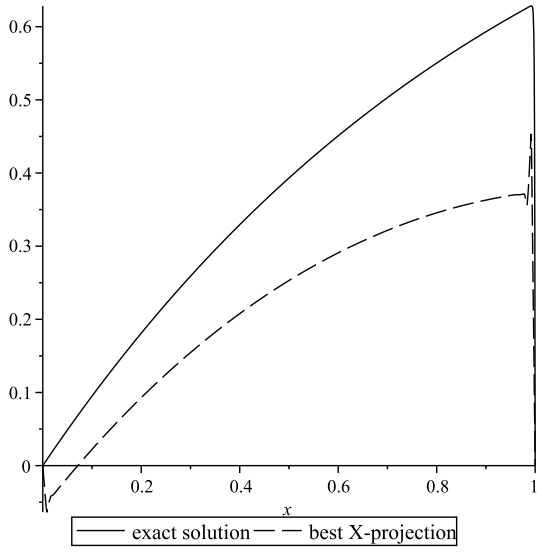


FIGURE 2. Exact solution and best X-projection onto piecewise linears with uniform mesh size 2^{-7} of the model problem (4.1).

4.1. Analysis of a 1d model problem

In spite of tight lower and upper *a posteriori* bounds the standard refinement strategies do apparently not necessarily imply a constant error reduction per step. To understand this better we consider a simple $1D$-example shown in Figure 2.

$$-10^{-3}u'' + u' + u = 1, \quad \text{on } (0,1), \quad u(0) = u(1) = 0. \tag{4.1}$$

As it will be seen, the issue we are facing is actually not directly related to specific adaptive refinements. In fact, in the above example we can apply an explicit formula for the inverse R_Y^{-1} in (2.15) is equivalent to the perfectly stable choice $Y_h = Y$. In view of the remarks from Section 2.3, this ensures stability of a corresponding discretization for any choice of X_h. For simplicity we choose X_h as the space of piecewise linear finite elements on an equidistant mesh of mesh size $h = 2^{-7}$. Figure 2 displays an approximate solution, which is the numerical evaluation of the exact X-orthogonal projection of the exact solution to X_h. Perhaps two phenomena look somewhat surprising, namely the occurrence of an oscillation at the inflow boundary and a distinct downward shift of the approximate solution. The implications on the approximation error become even more pronounced for the analogous example with smaller diffusion

$$-10^{-5}u'' + u' + u = 1, \text{on } (0,1), \quad u(0) = u(1) = 0.$$

Again an exact computation of the Y'-scalar product gives rise to errors in the X-norm displayed in Table 1 showing that there is essentially no error reduction for the first ten (uniform) refinement steps in the X-norm. Of course, ten steps of *local* refinements cannot do better either.

The reasons for this behavior seem to be the following. On one hand, the error is very much concentrated in the layer region which is hardly affected as long as the layer is not resolved. This explains the poor error reduction for the grids under consideration. To understand the strange downward shift it is instructive to look at the following example

$$-\epsilon u'' + bu' = f \quad \text{on } (0,1), \quad u(0) = u(1) = 0, \tag{4.2}$$

https://doi.org/10.1051/m2an/2012003 Published online by Cambridge University Press

TABLE 1. Error in the X-norm. Here u_h and u_H are the best X-projections where the grid of u_h has one additional refinement level to the one of u_H. Additionally P_Y is the best Y-approximation to the discrete space of u_h.

#cells	$\|u-u_h\|_X$	$\frac{\|u-u_h\|_X}{\|u-u_H\|_X}$	$\|u-P_Y u\|_Y$
4	0.960		0.478
8	0.958	0.998	0.463
16	0.957	0.999	0.455
32	0.957	1.000	0.451
64	0.956	0.999	0.449
128	0.954	0.998	0.447
256	0.949	0.995	0.446
512	0.939	0.989	0.445

where we assume for simplicity that ϵ and b are constant. Straightforward calculations show that in this case, for $\|v\|_Y^2 = \epsilon\|v'\|_{L_2(0,1)}^2$, one has

$$\|v\|_X^2 = \epsilon\|v'\|_{L_2(0,1)}^2 + \frac{b^2}{\epsilon}\inf_{c\in\mathbb{R}}\|v-c\|_{L_2(0,1)}^2. \tag{4.3}$$

Obviously, the X-norm hardly sees any constant shift of the solution because constants in the heavily (for small ϵ) emphasized L_2-term are factored out. So apparently the projection chooses a shift that reduces the layer errors by trading a single high layer against two lower layers.

Thus, it is the particular nature of the norm $\|\cdot\|_X$ causes the shift effect observed above together with the difficulty of quickly resolving the layer which seems to be necessary for error reduction with respect to this norm. Also it is clear that the shift effect is stronger when the equation does not involve any zero order term. Furthermore it seems that also the error of the best Y-projection is not reduced by a reasonable fixed constant so that this error does not become small on an affordable grid which does not resolve yet the layers. Note that this Y-norm is also contained in most other norms commonly used in connection with convection-diffusion problems as for example the norms of the SUPG-scheme. Thus in the given example such schemes might admit an error reduction but by Table 1 one cannot expect that the error becomes smaller than 0.44 for the given resolutions.

5. Modified variational formulations

The deficiencies observed above seem to be inherently connected with the constraints imposed by the variational formulation based on the standard choice. We shall therefore explore next modifications within the general framework described in Section 2. A possible guideline for finding suitable modifications is to search for variational formulations that allow us to stably pass the viscosity ϵ to zero. For the resulting *reduced problem* obtained in the limit case $\epsilon = 0$ one has to split the boundary $\Gamma = \partial\Omega$ into the pieces

$$\begin{aligned}\Gamma^+ &= \{x\in\Gamma:\ b\cdot n \geq 0\}\\ \Gamma^- &= \{x\in\Gamma:\ b\cdot n < 0\},\end{aligned} \tag{5.1}$$

where for any $x\in\Gamma$, $n = n(x)$ is the outward normal at x, Γ^- is the inflow boundary and Γ^+ stands for the outflow boundary (containing possibly characteristic boundary portions). Since the limiting PDE is a first order equation one can only prescribe boundary conditions on the inflow boundary Γ^- to obtain a well posed problem. Layers arising in the viscous problem are caused by the difference in admissible boundary conditions. This suggests to base modifications on a different way of incorporating boundary conditions.

https://doi.org/10.1051/m2an/2012003 Published online by Cambridge University Press

Depending on the variational formulations there seem to be two natural ways, being in some sense dual to each other, to impose these boundary conditions. Here we only give a short motivation and refer to [9] for a detailed discussion. A first natural weak formulation is obtained by integrating the reduced equation $b \cdot \nabla u + cu = f$ multiplyed by a test function which yields

$$\langle b \cdot \nabla u, v\rangle + \langle cu, v\rangle = \langle f, v\rangle\,. \tag{5.2}$$

Here $b\cdot\nabla u$ needs to belong to $L_2(\Omega)$ and under mild conditions on the velocity field b such functions are known to possess traces on the inflow and outflow boundary belonging to a weighted L_2-space on these boundary portions. This suggests to incorporate zero boundary conditions into the trial space on the the inflow boundary. For convection-diffusion problems, when viscosity is included, this gives rise to modified outflow boundary conditions to be discussed in Section 5.2.

An alternative variational setting for the reduced problem is obtained by applying integration by parts to the problem (5.2) which gives

$$\langle u, b\nabla v\rangle + \langle u, c - \mathrm{div}(bu)\rangle = \langle f, v\rangle + \int_{\partial\Omega} n\cdot b\gamma(u)\gamma(v), \tag{5.3}$$

where γ is the corresponding trace map. Prescribing $u_0 = \gamma_-(u)$ on Γ_- while imposing zero boundary conditions on Γ_+ for the test functions, the trace integral $\int_{\Gamma_-} n\cdot bu_0\gamma(v)$ becomes part of the right hand side functional which means that the Dirichlet conditions on Γ_- are natural boundary conditions that need not be built into the trial space. That this strategy gives indeed rise to a well-posed problem and additional details can be found in [9]. The modified treatment of boundary conditions for the convection-diffusion problem discussed next in Section 5.1 is based on the variational formulation (5.3) for the reduced problem where no boundary conditions are imposed on the test space.

5.1. Modifying inflow boundary conditions

Our point of departure is the standard bilinear form $a(\cdot,\cdot) = a_\circ(\cdot,\cdot)$ from (1.2) where $\hat{X}$ agrees with $H^1_0(\Omega)$. Motivated by (5.3) we choose, however, the test space $Y^+ = \{y \in H^1(\Omega) :\ u|_{\Gamma_+} = 0\}$ of functions which vanish only on the outflow boundary in the trace sense, endowed, for instance, with the norm $\|\cdot\|_Y$ given by (2.11). Thus, although $\|\cdot\|_{Y^+} = \|\cdot\|_Y$, we have $\|\cdot\|_{(Y^+)'} \neq \|\cdot\|_{Y'}$. With this new test space the variational problem: find $u \in \hat{X}$ such that

$$\langle Au, v\rangle = a_\circ(u, v) = \langle f, v\rangle\,, \quad v \in Y^+ \tag{5.4}$$

is over determined and in this form not well-posed. In fact, the right hand side of (5.4) is generally only well defined for $v \in H^1_0(\Omega)$. Therefore, the functional f has to be extended to the larger domain Y^+. With such an extension f^+ to Y^+ at hand, that will be specified below, and since the bilinear form $a_\circ(\cdot,\cdot)$ is well defined on $H^1_0(\Omega)\times H^1(\Omega)$ we can still employ a least squares formulation like (2.7) (see Rem. 2.1)

$$\|Au - f^+\|^2_{(Y^+)'} \to \min, \tag{5.5}$$

as the starting point for a numerical scheme. Of course, the operator $A : \hat{X} \to (Y^+)'$ defined by the first relation in (5.4) is not an isomorphism, but is is injective. Since A has a closed range it is, by the Closed Graph Theorem a an isomorphism from $\hat{X}$ to its range $(Y^+)'$. Therefore, the definition $\|v\|_X = \|Av\|_{(Y^+)'}$ of a graph norm as in (2.6) yields a complete space X, which agrees with $\hat{X}$ as a set, and renders the isomorphism perfectly well conditioned.

Returning to example (4.2) from the previous section, note that the X-norm as defined in (2.5) corresponding to the new test space Y^+ is

$$\|v\|^2_X = \epsilon\|v'\|^2_{L_2(0,1)} + \frac{b^2}{\epsilon}\|v\|^2_{L_2(0,1)}.$$

https://doi.org/10.1051/m2an/2012003 Published online by Cambridge University Press

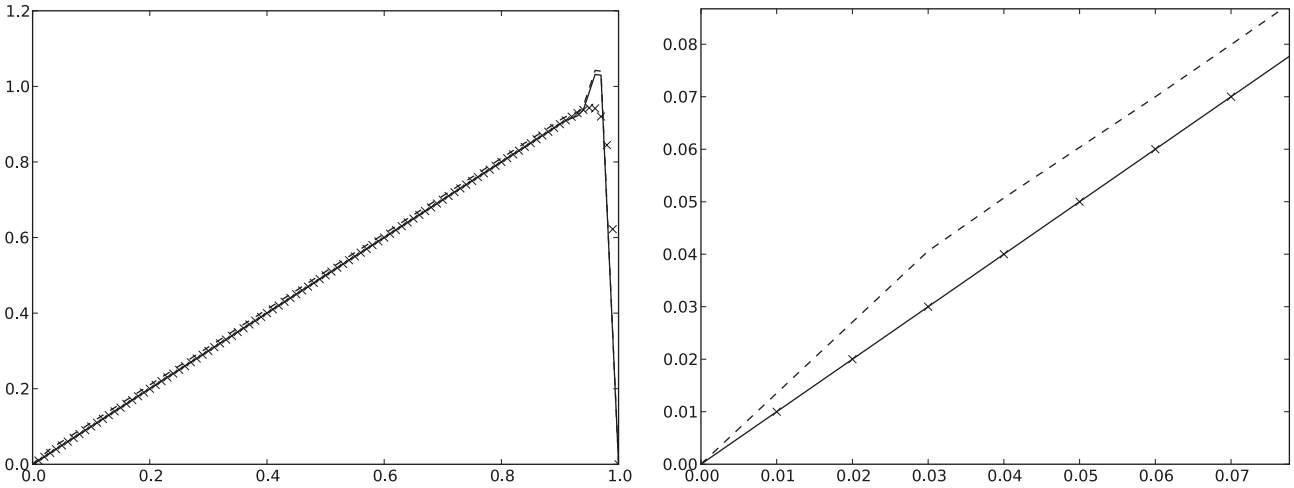


FIGURE 3. Solution of the model problem (4.2) by the systems (5.6) (dashed line) and (5.9) (solid line) for $\epsilon = 10^{-2}$ and $b = 1$. The "×" show the true solution. The right picture is a zoom into the lower left corner of the left picture.

In contrast to (4.3), shifting the solution by a constant, is now strongly penalized in the norm $\|\cdot\|_X$.

As in Section 2.2 we may write the normal equations of (5.5) in block form as

$$\begin{aligned} \langle y, Av\rangle &= 0, \qquad && v \in X, \\ \langle Au, z\rangle - \langle R_{Y^+} y, z\rangle &= (f^+, z), && z \in Y^+. \end{aligned} \tag{5.6}$$

Since $R_{Y^+} : Y^+ \to (Y^+)'$ is an isometry and since the test function $z := R_{Y^+}^{-1} Av$ shows that

$$\sup_{z\in Y^+} \frac{\langle z, Av\rangle}{\|v\|_X \|z\|_{Y^+}} \geq \frac{\langle R_{Y^+}^{-1} Av, Av\rangle}{\|v\|_X \|R_{Y^+}^{-1} Av\|_{Y^+}} = \frac{\|Av\|^2_{(Y^+)'}}{\|v\|_X \|Av\|_{(Y^+)'}} = 1,$$

the saddle point problem (5.6) is perfectly well conditioned and has a unique solution.

Once we have fixed f^+ we can apply the numerical techniques from the previous sections to (5.6) which is equivalent to solving the least squares problem (5.5). So it remains to specify f^+. When f happens to belong to $L_2(\Omega)$ it can be identified with a bounded functional in $(Y^+)'$ so we could simply take $f = f^+$ and the dual pairing $\langle f, v\rangle$ reduces to the L_2-scalar product. The numerical example is presented in Figure 3 explores this case. We see that the shift problem greatly benefits from the modification of the test space. However, there is still a small upwards shift left. In numerical experiments this shift is of the order of ϵ.

Since we have imposed some (mild) additional assumptions on the right hand side and because the shift problem is not completely resolved, the remainder of this section is devoted to the discussion of an alternative choice for the extension f^+.

An admissible extension is necessarily the result of a projection $E : Y' \to (Y^+)'$ so that its adjoint given by $\langle Ef, v\rangle = \langle f, E^* v\rangle$ is a Y-bounded projection from Y^+ onto Y, which agrees with $H_0^1(\Omega)$ as a vector space. Note that for A defined above one has for any $v \in Y^+$

$$\langle Au, v - E^* v\rangle = \langle Ef, v - E^* v\rangle = \langle Ef, v\rangle - \langle Ef, v\rangle = 0. \tag{5.7}$$

Here is a general construction of E. Assume that $a_e(\cdot,\cdot) : H^1(\Omega) \times H^1(\Omega) \to \mathbb{R}$ is a continuous bilinear form that is coercive on $H_0^1(\Omega)$. For instance, $a_\circ(\cdot,\cdot)$, given by (1.2) or also its symmetric part $a_s(\cdot,\cdot)$ qualify. This

https://doi.org/10.1051/m2an/2012003 Published online by Cambridge University Press

induces an isomorphism $A_e : H_0^1(\Omega) \to H^{-1}(\Omega) = (H_0^1(\Omega))'$. Defining E by $\langle Ef, v\rangle = a_e(A_e^{-1}f, v)$ yields an extension with the desired properties, where we make use of the fact that, although for the inversion of A_e we made use of the $H_0^1(\Omega)$-ellipticity, *i.e.* we used the zero boundary conditions, the bilinear form $a_e(\cdot,\cdot)$ is still well defined for all functions in $H^1(\Omega)$. In particular, the choice $a_e(\cdot,\cdot) = a_0(\cdot,\cdot)$ may appear somewhat tautological. Nevertheless, on the finite dimensional level discretizations are different. In order to exploit this effect without possibly realizing E explicitly let us first write the system (5.6) in a slightly different but equivalent form. Noting the second line in (5.6) as

$$\begin{aligned}\langle Au, E^*z\rangle - \langle R_{Y^+}y, E^*z\rangle &= \langle f, E^*z\rangle + \langle R_{Y^+}y, (I-E^*)z\rangle - \langle Au, (I-E^*)z\rangle \\ &= \langle f, E^*z\rangle + \langle R_{Y^+}y, (I-E^*)z\rangle\,,\end{aligned}$$

where we have used (5.7) in the last step, we can rewrite (5.6) equivalently as

$$\begin{aligned}\langle y, Av\rangle &= 0, && v \in X \\ \langle Au, z\rangle - \langle R_{Y^+}y, z\rangle &= \langle f, z\rangle\,, && z \in Y = E^*Y^+ \\ -\langle R_{Y^+}y, z\rangle &= 0, && z \in Y^c := (I-E^*)Y^+.\end{aligned} \tag{5.8}$$

Now, let $Y_h^+ \subset Y^+$ be any finite dimensional subspace and suppose that $Y_h^+ = Y_h \oplus Y_h^c$, where $Y_h \subset H_0^1$ and Y_h^c is any complement of Y_h into Y_h^+. Then a discretized counterpart to (5.8) reads: find $u_h \in X_h$ and $y_h \in Y_h^+$ such that

$$\begin{aligned}\langle y_h, Av_h\rangle &= 0, && v_h \in X_h \\ \langle Au_h, z_h\rangle - \langle R_{Y^+}y_h, z_h\rangle &= \langle f, z_h\rangle\,, && z_h \in Y_h \\ -\langle R_{Y^+}y_h, w_h\rangle &= 0, && w_h \in Y_h^c.\end{aligned} \tag{5.9}$$

Note that for the true solution u of the original variational problem $\langle Au, z\rangle = \langle f, z\rangle$ for all $z \in Y$ the second and third block row give $\langle R_{Y^+}y_h, z_h\rangle = 0$ for all $z_h \in Y_h^+$ which yields $y_h = 0$ so that this system is indeed consistent with the original problem.

Figure 4 shows the results of the variant (5.9) for the problems and numerical schemes described in Sections 3.4 and 3.3, respectively. In our experiment the space Y_h^c is simply the span of all finite element basis functions for the Y_h grid with nodes located on Γ^+. We see that the shift has disappeared completely, the grid is well adapted to the solution and this time there is no unphysical additional layer. Nevertheless, at an early refinement stage the oscillations in the layer region still look unnecessarily strong. However, one should note that they disappear as soon as the refinement level permits a layer resolution. More importantly, it seems that the intermediate oscillations do not mislead the refinement process. In this sense the scheme is stable. Moreover, the particular form (2.13) suggests that oscillations in transversal direction to the streamlines are primarily penalized in the dual norm $\|\cdot\|_{Y'}$ that permits them to some extent. In order to address the behavior prior to the layer resolution we shall explore next further alternatives.

5.2. Modifying the outflow boundary conditions

Motivated by the weak formulation (5.3) we have modified in the previous section the inflow boundary conditions of the test space which completely cures the shift artifact. However, still some oscillations in the layer region appear at early refinement stages. While they not seem to deceive adaptive refinements they also disappear earlier than in the initial standard formulation. To further reduce these oscillations recall that the trial spaces for the weak formulation (5.2) of the reduced problem are subject to boundary conditions only on the inflow boundary not on the outflow boundary. Accordingly, for the convection diffusion equation we employ next $X^- := \{u \in H^1(\Omega) : u|_{\Gamma^-\cup\Gamma_0} = 0\}$ as trial space. Since the zero boundary conditions on the outflow boundary are no longer built into the space X^- we impose them weakly. To explain this, we continue to denote by X, Y the Hilbert spaces that are equivalent to $H_0^1(\Omega)$ endowed with the norms $\|\cdot\|_X, \|\cdot\|_Y$, defined in Section 2.1, respectively. Let $\bar{A}$ be defined by $\langle \bar{A}v, w\rangle = a_\circ(v, w)$, $v \in X^-$, $w \in Y$, while $A : X \to Y$ is still

https://doi.org/10.1051/m2an/2012003 Published online by Cambridge University Press

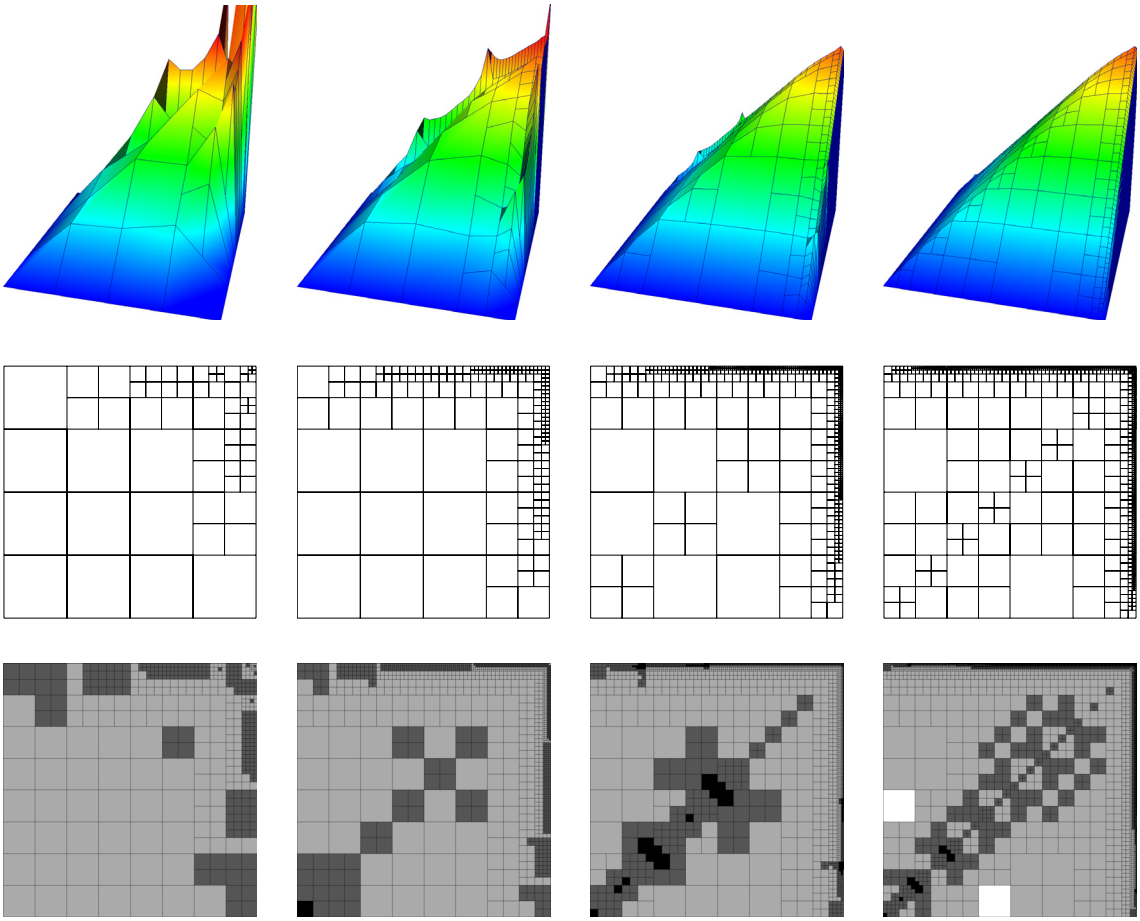


FIGURE 4. These pictures show every third adaptive cycle of Algorithm 1 with the above modification of the inflow boundary condition and $\epsilon = 5 \times 10^{-2}$, starting from cycle 5 for the test problem (3.25). The first row depicts the finite element solution u_h. The second row displays the corresponding grids of u_h. The third row shows the local amount j of refinement of the Y_h grid compared to the X_h grid (white $j = 0$, light grey $j = 1$, dark grey $j = 2$, black $j = 3$).

defined by $\langle Av, w\rangle = a_\circ(v, w)$, $v, w \in H_0^1(\Omega)$. Hence, $\bar{A}v = Av$ for $v \in X$. Furthermore, note that the trace map $\gamma : X^- \to H_{00}^{1/2}(\Gamma^+)$ is continuous and surjective. We shall endow $H_{00}^{1/2}(\Gamma^+)$ with a norm $\|\cdot\|_{Y_b}$ which will be specified later. For example, one could think of

$$\|g\|_{Y_b} := \inf_{w \in X^- : \gamma w = g} \|w\|_Y. \tag{5.10}$$

Now we consider the problem: find $u \in X^-$ such that

$$\|\bar{A}u - f\|_{Y'}^2 + \mu \|\gamma u\|_{Y_b}^2 \to \min, \tag{5.11}$$

where $\mu > 0$ is fixed. In order to apply the theory of Section 2, define

$$A^- : X^- \to Y' \times Y_b, \quad A^- u = [\bar{A}u, \gamma u],$$

https://doi.org/10.1051/m2an/2012003 Published online by Cambridge University Press

and set $\|[f,g]\|^2_{Y'\times Y_b} := \|f\|^2_{Y'} + \mu\|g\|^2_{Y_b}$. Then the least squares problem (2.7) applied to the pair of spaces $X^-, Y^- := Y \times Y_b'$ is equivalent to (5.11). To see that A^- is indeed an isomorphism, we first characterize the kernel of $\bar{A}$.

Proposition 5.1. *Let*

$$K := \{u \in X^- : \langle \bar{A}u, v\rangle = 0 \text{ for all } v \in Y\}$$

be the kernel of $\bar{A}$. Then K is nontrivial and the restriction $\gamma : K \to Y_b$ is an isomorphism.

Proof. Obviously, the trace operator γ is bounded. In order to show that its restriction to K is an isomorphism we construct an explicit inverse. To this end, for any $g \in Y_b$ let $w_g \in X^-$ denote the minimizer in (5.10). Let $z \in H^1_0(\Omega)$ be the unique solution of

$$a_\circ(z,v) = -a_\circ(w_g, v), \quad v \in H^1_0(\Omega)$$

and define $\delta(g) := z + w_g$. Then by construction, we have $\delta(g) \in K$ and $(\gamma\circ\delta)(g) = g$ for all $g \in Y_b$ and therefore γ is surjective. On the other hand, if $u \in K$ is such that $\gamma(u) = 0$ then $u \in H^1_0(\Omega)$ and $\bar{A}u = 0$ so that $u = 0$. Therefore γ is a bijection from K to Y_b. By the open mapping theorem, its inverse is bounded. □

Proposition 5.2. *The operator $A^- : X^- \to Y' \times Y_b$ is an isomorphism.*

Proof. Suppose that $A^-u = 0$. Since then, in particular, $\gamma u = 0$ we conclude that $u \in H^1_0(\Omega)$. Since $\langle \bar{A}u, v\rangle = a_\circ(u,v) = 0$ for all $v \in H^1_0$ implies $u = 0$ we see that A^- is injective.

In order to show that A^- is surjective, let $[f,g] \in Y' \times Y_b$. According to Proposition 5.1 there is a $w \in K$ with $\gamma w = g$. Furthermore there is a $u_0 \in H^1_0(\Omega)$ such that $a_0(u_0, v) = \langle f, v\rangle$, $v \in H^1_0(\Omega)$, which means that $\bar{A}u_0 = f$. Since K is the kernel of $\bar{A}$ we get $A^-(u_0 + w) = [f,g]$.

Obviously A^- is bounded. Since it is also surjective the inverse is bounded because of the open mapping theorem. □

The next proposition ensures that the solutions of the least squares problem (5.11) agrees with the solutions of the original convection-diffusion problem.

Proposition 5.3. *$u \in X$ satisfies $a_\circ(u,v) = \langle f, v\rangle$ for all $v \in Y$ if and only if one has for any positive μ*

$$u = \operatorname{argmin}_{v\in X^-} \{\|\bar{A}v - f\|^2_{Y'} + \mu\|\gamma v\|^2_{Y_b}. \tag{5.12}$$

Proof. Given $f \in Y'$ let $\tilde{u} \in X$ denote the solution of $a(\tilde{u}, v) = \langle f, v\rangle$, $v \in Y$ so that

$$\bar{A}\tilde{u} = A\tilde{u} = f \in Y', \quad \gamma\tilde{u} = 0.$$

Hence

$$0 = \|\bar{A}\tilde{u} - f\|^2_{Y'} + \mu\|\gamma\tilde{u}\|^2_{Y_b}$$

and $\tilde{u}$ is a minimizer of $\{\|\bar{A}v - f\|^2_{Y'} + \mu\|\gamma v\|_{Y_b}\}$. Conversely, since the minimal value of the functional is zero, any minimizer u must have a zero trace on Γ^+ and must therefore satisfy $\bar{A}u = Au = f$, which completes the proof. □

Now we can apply the theory developed in Section 2 to the equivalent problem $A^-u = [f, 0]$. Then, according to (2.6), for each parameter μ the graph-norm for the space X^- takes the form

$$\|u\|^2_{X^-} := \|\bar{A}u\|^2_{Y'} + \mu\|\gamma u\|^2_{Y_b},$$

and assures that the operator $A^- : X^- \to Y' \times Y_b$ has condition number $\kappa_{X^-, Y\times Y_b'}(A^-)$ equal to one.

https://doi.org/10.1051/m2an/2012003 Published online by Cambridge University Press

While the actual value of the parameter $\mu > 0$ is irrelevant for the infinite dimensional problem it does matter for discretizations based on the above least squares formulation. We postpone this issue for a moment and turn first to suitable variational formulations of the least squares problem (5.11) for a given $\mu > 0$. These can now be derived by applying the machinery of Section 2.2. To this end, let $X_h^- \subset X^-$ and $Y_h \subset Y$ be finite dimensional subspaces. For the boundary component, we choose first the full infinte dimensional space Y_b'. Then application of the theory of Section 2.2 the system (2.26) takes here the form: find $u_h \in X_h^-$ and $[y_h, g] \in Y_h \times Y_b'$ such that

$$\begin{aligned} \langle y_h, \bar{A} v_h \rangle + \langle g, v_h \rangle &= 0, \qquad && v_h \in X_h^-, \\ \langle \bar{A} u_h, z_h \rangle + \langle u_h, q \rangle - \langle R_Y y_h, z_h \rangle - \mu^{-1} \langle R_{Y_b}^{-1} g, q \rangle &= \langle f, z_h \rangle, && [z_h, q] \in Y_h \times Y_b'. \end{aligned} \tag{5.13}$$

Here, R_{Y_b} is the Riesz map for the Y_b-scalar product which is then given by $\langle R_{Y_b} \cdot, \cdot \rangle$. As an example, one could take the standard scalar product for $H_{00}^{1/2}(\Gamma_-)$. The practical drawback is that this system involves the inverse of the Riesz-map R_{Y_b} since the system was designed for least squares problems which minimize the residual in a dual norm. For the current problem, this is not entirely true since the residual for the boundary terms is measured in a primal norm. To make use of this observation, note first that the normal equation for the optimization problem (5.11) is equivalent to: find $u \in X^-$ s.t.

$$\langle \bar{A} u - f, \bar{A} v \rangle_{Y'} + \mu \langle u, v \rangle_{Y_b} = 0, \quad v \in Y.$$

This suggests applying the reasoning in Section 2.2 only to the first summand while leaving the second one unchanged. This yields the simpler system: find $u \in X_h^-$ and $y \in Y_h$ s.t.

$$\begin{aligned} \mu \langle u_h, v_h \rangle_{Y_b} + \langle y_h, A v_h \rangle &= 0, \qquad && v_h \in X_h^- \\ \langle A u_h, z_h \rangle - \langle R_Y y_h, z_h \rangle &= \langle f, z_h \rangle, && z_h \in Y_h. \end{aligned} \tag{5.14}$$

The next lemma shows that the two systems (5.13) and (5.14) are equivalent.

Lemma 5.4. *Let u_h and y_h be solutions of the system (5.14). Then there is a $g \in Y_b'$ such that u_h, y_h and g solve the system (5.13).*

Conversly if u_h, y_h and g solve the system (5.13) then u_h and y_h also solve (5.14).

Proof. Let $u_h, [y_h, g]$ be the solutions of the system (5.13). Considering the last equation of this system for $z_h = 0$, we obtain

$$\langle u_h, h \rangle - \mu^{-1} \langle R_{Y_b}^{-1} g, h \rangle_{Y_b} = 0, \quad h \in Y_b, \tag{5.15}$$

i.e. $g = \mu R_{Y_b} \gamma u_h$. Plugging this into (5.13) and setting $h = 0$, we find that u_h and y_h also solve the system (5.14).

Conversely, let u_h and y_h be the solution of (5.14). Then for g defined by (5.15) the functions u_h and $[y_h, g]$ solve the system (5.13). □

Recall that the specific structure of the *a-posteriori* error estimators in Section 3 results from the fact that the residual of the least squares problem in Remark 2.1 is measured in a dual norm which is generally difficult to evaluate. The same dual norm still occurs in the optimization problem (5.11). Therefore we can apply the same techniques of Section 3 to derive *a-posteriori* error estimators for the modified scheme as well.

We now turn to the choice of μ in the system (5.14). As seen before, since in the infinite dimensional case the minimal value of the least squares functional is zero, μ can be chosen arbitrarily in (5.12). However, as soon as one uses a discretization the residual $\bar{A} u_h - f$ no longer vanishes in Y' and the choice of μ determines the balance between the trace residual in an $H^{1/2}$-like norm and $\|\bar{A} u_h - f\|_{Y'}$. It is instructive to consider the two extreme cases. Letting μ tend to infinity would enforce homogeneous boundary conditions in the finite dimensional trial spaces. Hence, very large values of μ are expected to give rise to solutions exhibiting shift artifacts. On the other hand, choosing $\mu = 0$ in the infinite dimensional problem the operator A^- has a nontrivial kernel characterized

https://doi.org/10.1051/m2an/2012003 Published online by Cambridge University Press

by Proposition 5.1. One possible solution of the least squares problem (5.11) is $u^{\rm dir}$ is the one of the original convection-diffusion problem (1.2). However, since we do not impose any boundary conditions on the outflow we expect in addition the existence of solutions which have no layers at all. For example, the solution $u^{\rm neu}$ satisfying Neumann boundary conditions at the outflow is one candidate. Generally, we expect that $u^{\rm neu}$ can be approximated well whereas the boundary layer of $u^{\rm dir}$ severely impedes on the quality of an approximate solution. Denoting by $u_h^{\rm dir}$ and $u_h^{\rm neu}$ approximations to $u^{\rm dir}$ and $u^{\rm neu}$, respectively, from the finite dimensional space X_h^-, we therefore expect $\|\bar{A}u_h^{\rm dir} - f\|_{Y'}$ to be significantly larger than $\|\bar{A}u_h^{\rm dir} - f\|_{Y'}$. By the definition of the X^- norm, the same holds for the approximation error in this norm. Hence, without any trace penalization, *i.e.* for $\mu = 0$, the minimization of (5.11) over the finite dimensinal spaces X^- would favor $u_h^{\rm neu}$ over $u_h^{\rm dir}$. Furthermore, note that

$$u^{\rm ker} := u^{\rm dir} - u^{\rm neu} \tag{5.16}$$

is expected to differ significantly from zero only in the layer region so that $u_h^{\rm neu}$ is still a good approximation of the given convection-diffusion problem (1.2) away from the layer region. Moreover, as long as the layer is not resolved the approximation quality remains very poor in the layer region anyway so that the solution quality elsewhere may actually benefit from ignoring the boundary conditions on Γ^+. A qualitatively similar behavior is expected to persist for very small μ. With increasing resolution of X_h^- the residual $\|\bar{A}u_h - f\|_{Y'}$ will eventually be small enough so that the trace term $\mu\|\gamma u_h\|_{Y_b}$ becomes important and the numerical solution u_h will tend to become more similar to $u_h^{\rm dir}$. In summary, a desirable behavior of a numerical scheme would be to produce approximations close to $u^{\rm neu}$ as long as the layer is not resolved while beyond that point $u^{\rm dir}$ is approximated. To achieve this both terms in the least squares functional should be roughly balanced. Since by the above reasoning, for $\|\cdot\|_X$ given by (2.13),

$$\|\bar{A}u_h - f\|_{Y'} \sim \|u - u_h\|_X \sim \|u^{\rm ker}\|_X$$

and since the effect of $\|\cdot\|_X$ on the layer is similar to that of $\|\cdot\|_Y$, the specification (5.10) calls for the choice $\mu = 1$. Neglecting the zero order term in the convection diffusion operator, one obtains essentially $\|\cdot\|_Y = \sqrt{\epsilon}|\cdot|_{H^1}$ so that $\|\cdot\|_{Y_b}$ becomes essentially $\sqrt{\epsilon}\|\cdot\|_{H^{1/2}(\Gamma^+)}$. Since in tangential direction to Γ^+ the solution varies smoothly we have replaced in a first numerical experiment $\|\cdot\|_{H^{1/2}(\Gamma^+)}$ for simplicity by a (mesh size-) weighted $\|\cdot\|_{L_2(\Gamma^+)}$-norm. Figure 5 shows the results for the problem and adaptive scheme described in Section 3.4 with the modifications of the present section. For the viscosity $\epsilon = 10^{-5}$ Figure 5 displays refinements that cannot resolve the layer. Yet, this time neither oscillations nor refinements near the layer region occur while away from the layer region excellent accuracy is observed. It will be shown in the next section that one can nevertheless still derive accurate information about gradients in the layer.

Figure 6 shows for $\epsilon = 5 \times 10^{-3}$ what happens when the local refinements permit to resolve the layer. Already for the above simple choice of the penalty parameter μ the resolution of the layer is triggered automatically and the layer is finally resolved. Note that when this transition in the refinement process starts a peaked overshoot occurs which immediately disappears in subsequent steps. This phenomenon is somewhat stronger when using the exact $H^{1/2}$-norm instead of the weighted L_2-norm.

5.3. Drag and lift

Of course, modifying the outflow boundary conditions, changes the problem. In this section we argue though that we can still retain some interesting information on the layers. In particular, we are interested in functionals of the form

$$l(u) = \epsilon \int_{\partial\Omega} n\nabla u w, \tag{5.17}$$

where $w \in H^{1/2}(\partial\Omega)$ and n is the outward normal vector. These functionals are a simple model for physical quantities like drag and lift coefficients in the case of fluid dynamics. It seems that, due to changing outflow boundary conditions in the last section, one has no useful information on such functionals in the layer regions. However, in this section we offer a heuristic argument for still estimating such functionals from the solutions

https://doi.org/10.1051/m2an/2012003 Published online by Cambridge University Press

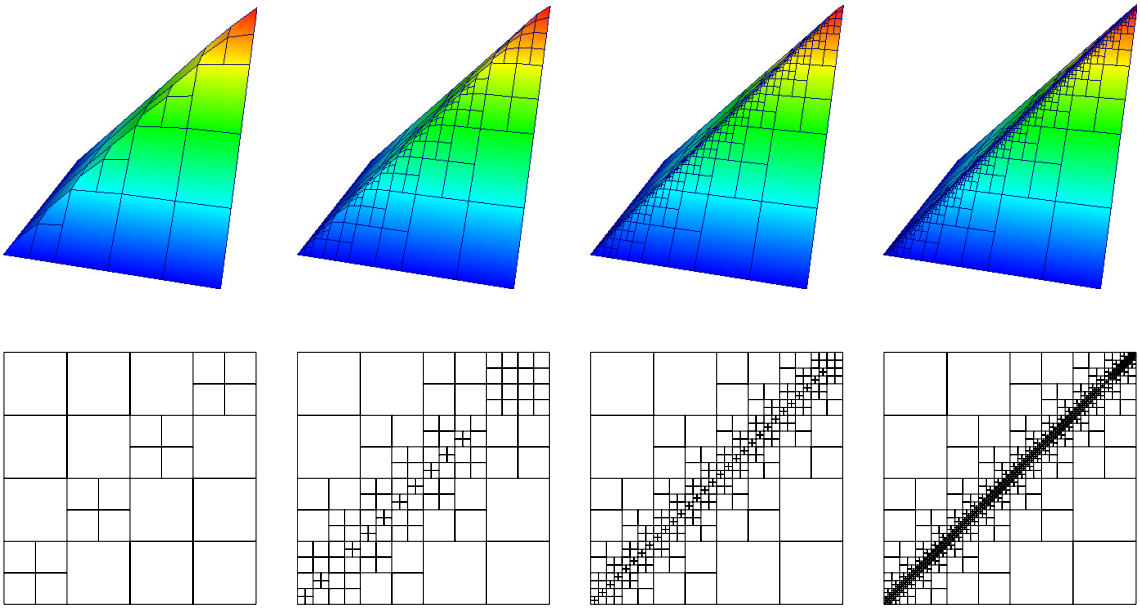


FIGURE 5. These pictures show every fourth adaptive cycle of Algorithm 1 with modification at the outflow boundary starting from cycle 3 for the test problem (3.25) with $\epsilon = 10^{-5}$. The first row depicts the finite element solution u_h. The second row displays the corresponding grids of u_h.

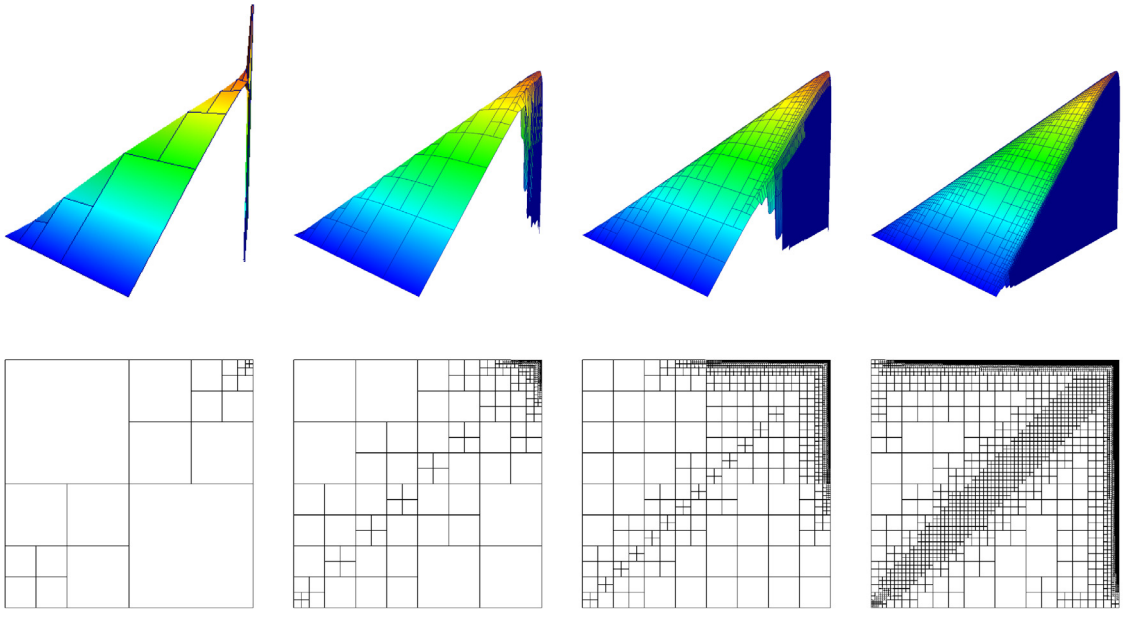


FIGURE 6. These pictures show every fourth adaptive cycle of Algorithm 1 with modification at the outflow boundary starting from cycle 3 for the test problem (3.25) with $\epsilon = 5 \times 10^{-3}$. The first row depicts the finite element solution u_h. The second row displays the corresponding grids of u_h.

https://doi.org/10.1051/m2an/2012003 Published online by Cambridge University Press

of the last section. For convenience we assume that the convection-diffusion problem is given in the alternative form

$$Au = -\epsilon \Delta u + \operatorname{div}(\tilde{b}u) + \tilde{c}u,$$

and that all quantities are sufficiently smooth. Recall that in Section 5.2 in (5.16) we have split the solution as $u^{\mathrm{dir}} = u^{\mathrm{neu}} + u^{\mathrm{ker}}$ where u^{dir} is the original solution with zero boundary conditions everywhere, u^{neu} is a solution with free outflow boundary conditions and u^{ker} is in the kernel of A. Thus, u^{ker} is specified by the equations

$$Au^{\mathrm{ker}} = 0 \qquad\qquad u^{\mathrm{ker}}|_{\partial\Omega} = -u^{\mathrm{neu}}|_{\partial\Omega}.$$

To evaluate the functional l from (5.17) the same splitting provides

$$l(u^{\mathrm{dir}}) = l(u^{\mathrm{neu}}) + l(u^{\mathrm{ker}}).$$

Recall that u^{neu} is the solution with the free outflow boundary conditions so that $l(u^{\mathrm{neu}})$ can be easily computed. Since generally we cannot resolve the boundary layer we cannot expect to compute $l(u^{\mathrm{ker}})$ directly. However, the following heuristics should offer a good estimator for this quantity. To this end, consider the harmonic extension w_e of w given by

$$-\Delta w_e = 0, \text{ in } \Omega, \quad w_e = w, \text{ on } \partial\Omega.$$

In the following we do not distinguish between w and its extension w_e and always write w. Then we get

$$l(u^{\mathrm{ker}}) = \epsilon \int_{\partial\Omega} n\nabla u^{\mathrm{ker}} w = -\epsilon \int_{\Omega} \operatorname{div}(\nabla u^{\mathrm{ker}} w) = -\epsilon \int_{\Omega} \Delta u^{\mathrm{ker}} w - \epsilon \int_{\Omega} \nabla u^{\mathrm{ker}} \nabla w = -S_1 - S_2.$$

Since, by definition, $\Delta w = 0$ we obtain

$$S_2 = \epsilon \int_{\Omega} \nabla u^{\mathrm{ker}} \nabla w = -\epsilon \int_{\Omega} u^{\mathrm{ker}} \Delta w + \epsilon \int_{\partial\Omega} n u^{\mathrm{ker}} \nabla w = \epsilon \int_{\partial\Omega} n u^{\mathrm{ker}} \nabla w.$$

Next we treat S_1. Because u^{ker} is in the kernel of A we have $\epsilon\Delta u^{\mathrm{ker}} = \operatorname{div}(\tilde{b}u^{\mathrm{ker}}) + \tilde{c}u^{\mathrm{ker}}$ which yields

$$\begin{aligned} S_1 &= \int_{\Omega} (\operatorname{div}(\tilde{b}u^{\mathrm{ker}}) + \tilde{c}u^{\mathrm{ker}}) w = \int_{\Omega} \operatorname{div}(\tilde{b}u^{\mathrm{ker}} w) - \int_{\Omega} \tilde{b}u^{\mathrm{ker}} \nabla w + \int_{\Omega} \tilde{c}u^{\mathrm{ker}} w \\ &= -\int_{\partial\Omega} n\tilde{b}u^{\mathrm{ker}} w - \int_{\Omega} \tilde{b}u^{\mathrm{ker}} \nabla w + \int_{\Omega} \tilde{c}u^{\mathrm{ker}} w. \end{aligned}$$

Putting the pieces together, we obtain

$$l(u^{\mathrm{dir}}) = \epsilon \int_{\partial\Omega} n\nabla u^{\mathrm{dir}} w = \epsilon \int_{\partial\Omega} n\nabla u^{\mathrm{neu}} w + \int_{\partial\Omega} n\tilde{b}u^{\mathrm{ker}} w + \int_{\Omega} \tilde{b}u^{\mathrm{ker}} \nabla w - \int_{\Omega} \tilde{c}u^{\mathrm{ker}} w - \epsilon \int_{\partial\Omega} n u^{\mathrm{ker}} \nabla w.$$

Since u^{ker} agrees with $-u^{\mathrm{neu}}$ on $\partial\Omega$ we can now compute the boundary integrals without knowing u^{ker} explicitly. For the remaining two summands one could argue as follows: since $Au^{\mathrm{ker}} = 0$ we expect u^{ker} to be close to zero except for some layer regions of width ϵ. Thus, neglecting these terms, we obtain the following approximation to l, given by

$$l_h([u,\sigma]) = \epsilon \int_{\partial\Omega} n\nabla u^{\mathrm{neu}} w - \int_{\partial\Omega} n\tilde{b}u^{\mathrm{neu}} w + \epsilon \int_{\partial\Omega} n u^{\mathrm{neu}} \nabla w.$$

This estimate might also be interesting from the perspective of turbulence modeling. There one of the leading questions is to what extend one can extract information on the unresolved scales from the resolved ones. In a much simpler model this is exactly what this estimator is doing: it can estimate the gradient in the layer region without resolving it.

As a simple example we use the model problem (3.25) with rigth hand side

$$u(x,y) = xy\left(1 - \exp\left(-\frac{1-x}{\epsilon}\right)\right)\left(1 - \exp\left(-\frac{1-y}{\epsilon}\right)\right).$$

Table 2 shows the exact error of the estimation of the boundary integral $\int_{\partial\Omega} n\nabla u$.

https://doi.org/10.1051/m2an/2012003 Published online by Cambridge University Press

TABLE 2. Error of estimation of the boundary integral $\int_{\partial\Omega} n\nabla u$.

Adaptive cycle	$\epsilon = 5 \times 10^{-2}$	$\epsilon = \times 10^{-5}$	Adaptive cycle	$\epsilon = 5 \times 10^{-2}$	$\epsilon = \times 10^{-5}$
1	4.99e-01	9.51e-06	8	1.49e-01	9.95e-06
2	2.79e-01	9.99e-06	9	1.14e-01	9.91e-06
3	2.77e-01	9.99e-06	10	8.80e-02	9.89e-06
4	2.28e-01	9.98e-06	11	7.70e-02	9.88e-06
5	2.40e-01	9.98e-06	12	5.21e-02	9.87e-06
6	2.23e-01	9.97e-06	13	4.33e-02	9.78e-06
7	1.71e-01	9.96e-06	14	3.39e-02	9.69e-06

6. CONCLUSION

We have proposed and analyzed adaptive numerical schemes for convection-diffusion problems based on a uniformly well-posed variational formulation that gives rise to a mapping property. The main example are the norms used by Sangalli and Verfürth in [19, 21]. To construct a numerical scheme which finds near best approximations in these norms we introduce an auxiliary variable whose resolution compared to the resolution of the solution itself determines the amount of stabilization. We have developed *a-posterior* conditions that ensure a sufficient resolution of this auxiliary variable adaptively. Together with the *a-posteriori* error estimators developed in this paper this yields a new adaptive scheme for convection-diffusion problems where, in contrast to earlier work, the norms used in the derivation of the error indicators agree with the norms in which accuracy is measured.

However, first numerical tests reveal the fact that for the "standard" variant the chosen norms tend to create – perhaps unexpected – artifacts in the numerical solution. It is perhaps somewhat surprising, at least at the first glance, that a uniformly stable variational formulation together with reliable and efficient *a-posteriori* bounds do not automatically guarantee error histories exhibiting a quantitatively "ideal" behavior. More involved discretizations like hp- or anisotropic refinements would certainly diminish the observed adverse effects. We have not pursued this line here. Instead, to understand the principal phenomena concerning the interplay between adaptivity and stability has been a core objective of the present work. Here, two remedies have been presented. Guided by the reduced problem with vanishing viscosity, one can modify the boundary conditions either at the inflow or outflow boundary to obtain norms which do no longer give rise to those artifacts. As long as the layer is not resolved oscillations still appear for low resolution in the first case which, however, remain within the layer region and do not mislead further mesh refinements. In the latter case the layer is no longer present and one obtains very accurate oscillation free solutions away from the layer region before the layer is resolved. An interesting point to be explored further is that one can still gain, somewhat in the spirit of subcell resolution, very accurate information on gradients in this region as is needed, for instance, for the computation of relevant functionals of the solution such as drag and lift.

REFERENCES

[1] J.H. Bramble and J.E. Pasciak, A new approximation technique for div-curl systems. *Math. Comp.* **73** (2004) 1739–1762.
[2] J.H. Bramble, R.D. Lazarov and J.E. Pasciak, Least-squares methods for linear elasticity based on a discrete minus one inner product. *Comput. Methods Appl. Mech. Eng.* **191** (2001) 727–744.
[3] F. Brezzi and M. Fortin, Mixed and Hybrid Finite Element Methods. Springer Series in *Comput. Math.* **15** (1991).
[4] F. Brezzi, T.J.R. Hughes, L.D. Marini, A. Russo and E. Süli, *A priori* analysis of residual-free bubbles for advection-diffusion problems. *SIAM J. Numer. Anal.* **36** (1999) 1933–1948.
[5] A. Cohen, W. Dahmen and R. DeVore, Adaptive wavelet methods II – beyond the elliptic case. *Found. Comput. Math.* **2** (2002) 203–245.
[6] A. Cohen, W. Dahmen and R. DeVore, Adaptive wavelet schemes for nonlinear variational problems. *SIAM J. Numer. Anal.* **41** (2003) 1785–1823.
[7] S. Dahlke, W. Dahmen and K. Urban, Adaptive wavelet methods for saddle point problems – convergence rates. *SIAM J. Numer. Anal.* **40** (2002) 1230–1262.

https://doi.org/10.1051/m2an/2012003 Published online by Cambridge University Press

[8] W. Dahmen, S. Müller and T. Schlinkmann, On an adaptive multigrid solver for convection-dominated problems, *SIAM J. Sci. Comput.* **23** (2001) 781–804.

[9] W. Dahmen, C. Huang, C. Schwab and G. Welper, *Adaptive Petrov-Galerkin methods for first order transport equations*. IGPM Report 321, RWTH Aachen (2011).

[10] L. Demkowicz and J. Gopalakrishnan, A class of discontinuous Petrov-Galerkin methods. Part II: Optimal test functions. *Numer. Methods Partial Differ. Equ.* **27** (2011) 70–105.

[11] L. Demkowicz and J. Gopalakrishnan, A class of discontinuous Petrov-Galerkin methods. Part III: Adaptivity. To appear in *Appl. Numer. Math.* (2012).

[12] J.L. Guermond, J.T. Oden and S. Prudhomme, An interpretation of the Navier-Stokes-alpha model as a frame-indifferent Leray regularization. *Physica D* **177** (2003) 23–30.

[13] J.-L. Guermond, J.T. Oden and S. Prudhomme, Mathematical perspectives on large eddy simulation models for turbulent flows. *J. Math. Fluid Mech.* **6** (2004) 194–248.

[14] T. Hughes and G. Sangalli, Variational multiscale analysis: the fine-scale Green's function, projection, optimization, localization, and stabilized methods. *SIAM J. Numer. Anal.* **45** (2007) 539–557.

[15] V. John, S. Kaya and W. Layton, A two-level variational multiscale method for convection-diffusion equations. *Comput. Methods Appl. Mech. Eng.* **195** (2006) 4594–4603.

[16] E. Lee and T.A. Manteuffel, FOSLL* method for the eddy current problem with three-dimensional edge singularities. *SIAM J. Numer. Anal.* **45** (2007) 787–809.

[17] T. Manteuffel, S. McCormick, J. Ruge and J.G. Schmidt, First-order system $\mathcal{LL}^*$ $(FOSLL)^*$ for general scalar elliptic problems in the plane. *SIAM J. Numer. Anal.* **43** (2005) 2098-2120.

[18] G. Sangalli, A uniform analysis of non-symmetric and coercive linear operators. *SIAM J. Math. Anal.* **36** (2005) 2033–2048.

[19] G. Sangalli, Robust *a-posteriori* estimators for advection-diffusion-reaction problems. *Math. Comput.* **77** (2008) 41–70.

[20] R. Verfürth, Robust *a-posteriori* error estimators for a singularly perturbed reaction-diffusion equation. *Numer. Math.* **78** (1998) 479–493.

[21] R. Verfürth, Robust *a posteriori* error estimates for stationary convection-diffusion equations. *SIAM J. Numer. Anal.* **43** (2005) 1766–1782.

https://doi.org/10.1051/m2an/2012003 Published online by Cambridge University Press